AD-A068 788 ADMIRALTY MARINE TECHNOLOGY ESTABLISHMENT TEDDINGTON--ETC F/G 20/1
ESTIMATION OF THE RMS VALUE OF SUMMED SINUSOIDS AND THE APPLICA--ETC(U)
NOV 78 A W WALKER

UNCLASSIFIED AMTE(N)/TM78413 DRIC-BR-66838 NL

| OF |
AD
A068788

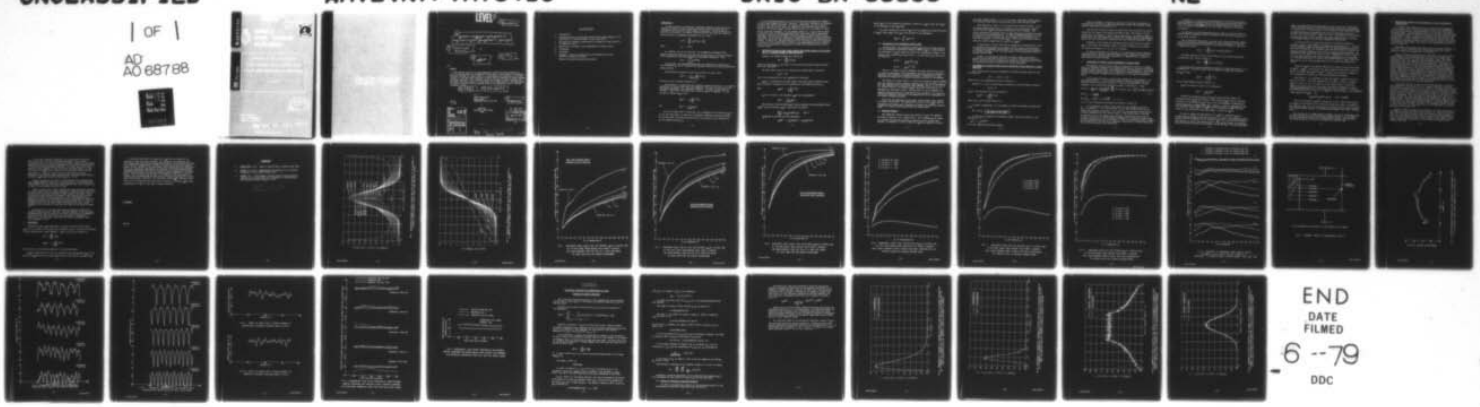

END
DATE FILMED
6 -79
DDC

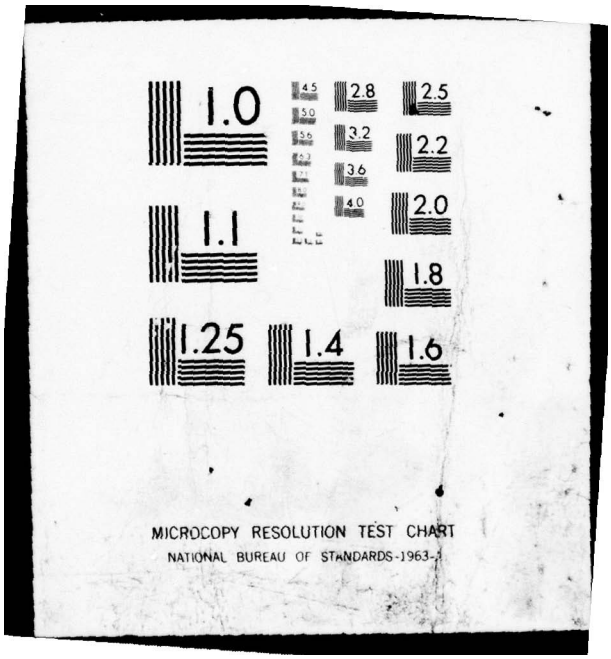
1.0
1.1
1.25
1.4
1.6
1.8
2.0
2.2
2.5
2.8
3.2
3.6
4.0
4.5
5.0
5.6
MICROCOPY RESOLUTION TEST CHART
NATIONAL BUREAU OF STANDARDS-1963-A

LEVEL II

(14) AMTE(N)/TM78413

(6) ESTIMATION OF THE RMS VALUE OF SUMMED SINUSOIDS AND THE APPLICATION TO ACOUSTIC NOISE MEASUREMENT IN SHALLOW WATER.

(9) Technical memo.

BY

(10) A. W. WALKER

(12) 38 pp

ABSTRACT

Summary

The spatial variation of many measurable quantities such as pressure or velocity may generally be synthesised by the sum of a given number of sinusoids. The power average of a small number of random samples is presented as a suitable estimate of the mean power contained in such a sum of sinusoids of random argument and equal amplitude. The confidence levels which apply to these estimates are presented, and the technique is illustrated by its application to the measurement of acoustic radiated noise in shallow water by the appropriate use of vertical transducer arrays.

(18) DRIC (19) BR-66838

ABSTRACT

AMTE (Teddington)
Queens Road
TEDDINGTON Middx TW11 OLN

(11) November 1978

42 pp
20 figs

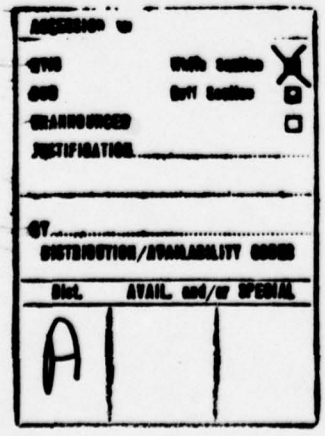

DDC
RECEIVED
MAY 9 1979
D

CONTENTS

INTRODUCTION

In many practical circumstances, measurable physical quantities such as pressure or velocity display significant spatial variations which may be represented by the sum of a given number of sinusoids. If the variation is periodic with period x_o the spatial variation may be described by a discrete Fourier series of fundamental wavenumber $2\pi/x_o$. Thus

$$p(x) = \sum_{m=1}^{M} a_m \sin(k_m x + \phi_m)$$

where $$k_m = 2\pi m/x_o$$

If, however, $p(x)$ is not periodic, the fundamental wavenumber $2\pi/x_o$ becomes vanishingly small and $p(x)$ may only be described by a Fourier integral which represents a continuous spectrum of wavenumber components. Thus

$$p(x) = \int_{-\infty}^{\infty} w(k) e^{ikx} dk$$

In this case, the sinusoidal components are harmonically unrelated and the wavenumbers k_m may be considered to represent values of an evenly distributed random variable.

The mean power contained in $p(x)$ may be defined by $G_M(x)$ where

$$G_M(x) = \lim_{N \to \infty} \frac{1}{N} \sum_{n=1}^{N} p^2(x_n)$$

where the x_n are N random locations of x.

Unfortunately, in cases where $p(x)$ defines a spatial variation, it is usually impractical to collect more than a few samples of the value of $p(x)$ since each new sample represents a new transducer location. In these circumstances an estimate of $G_M(x)$ must be derived from a limited number of samples. If this estimate is denoted $g_{NM}(x)$ then

$$g_{NM}(x) = \frac{1}{N} \sum_{n=1}^{N} p^2(x_n)$$

and $$G_M(x) = \lim_{N \to \infty} g_{NM}(x)$$

As will be shown later in this note, the convergence of the estimate $g_{NM}(x)$ to its true value $G_M(x)$ is rapid as N increases, enabling an accurate estimate of the mean power to be made using as few as ten values of $p(x_n)$ evaluated at the ten random locations x_n.

In the following analysis, all of the contributing sinusoids are assumed to have random arguments and unit amplitude. This latter assumption is necessary to render the problem tractable. In these circumstances, it will be shown in Section 2 that for a given number of samples N, the confidence which may be placed in the estimate $g_{NM}(x)$ reduces monotonically as M, the number of contributing sinusoids increases. For the special case M = 1, it will also be shown in Section 3 that increasing background noise levels also lead to significant monotonic reductions in confidence levels for signal to noise ratios of less than 20dB. For an infinite number of contributing sinusoids of equal amplitude, confidence levels have been determined by application of the chi-squared distribution. In Section 4, the applicability of the confidence levels is illustrated in relation to the enhancement of acoustic noise measurements taken in shallow water, by the appropriate processing of outputs from transducers which form a vertical array.

2. CONFIDENCE LIMITS FOR MEAN POWER DERIVED FROM RANDOM SAMPLES OF THE VECTOR SUM OF A VARIABLE NUMBER OF PURE SINE WAVES

Consider the random variable p(x) defined by

$$p(x) = \sum_{m=1}^{M} \sin(k_m x)$$

where the wavenumbers k_m are taken from an evenly distributed random variable such that $0 \leq k_m \leq \infty$.

The mean square value of p(x) which may be denoted $G_M(x)$ is given by

$$G_M(x) = \tfrac{1}{2}M$$

due to the orthogonality of the trigonometric functions.

$g_{NM}(x)$, an estimate of the mean square value $G_M(x)$ may be defined as the power average of N samples of p(x) evaluated at the random locations x_n.

Thus

$$g_{NM}(x) = \frac{1}{N} \sum_{n=1}^{N} p^2(x_n)$$

$G_M(x)$ is related to the estimate $g_{NM}(x)$ by the expression

$$G_M(x) = \lim_{N \to \infty} g_{NM}(x)$$

The accuracy of the estimate $g_{NM}(x)$ may be defined by the confidence level $L_{NM}(\alpha)$ that any estimate $g_{NM}(x)$ lies within the bounds

$$\frac{G_M(x)}{\alpha} \leq g_{NM}(x) \leq \alpha G_M(x), \qquad (\alpha > 1)$$

$L_{NM}(\alpha)$ may be derived from the expression

$$L_{NM}(\alpha) = C_{NM}(\alpha G_M(x)) - C_{NM}(G_M(x)/\alpha)$$

where $C_{NM}(y)$ is the cumulative probability function of $g_{NM}(x)$ such that $C_{NM}(y)$ is the probability that $g_{NM}(x) \leq y$.

It is also convenient to define $P_{NM}(x)$ as the probability density function of $g_{NM}(x)$ since $P_{NM}(x)$ and $C_{NM}(y)$ are related by the expression

$$C_{NM}(y) = \int_0^y P_{NM}(x)\, dx$$

2.1 Derivation of the confidence levels $L_{NM}(\alpha)$

As shown above, the confidence levels $L_{NM}(\alpha)$ may be derived directly from the appropriate probability density function $P_{NM}(x)$. Unfortunately the derivation of $P_{NM}(x)$ cannot be carried out analytically except in the special case in which both M and N are 1. In this case $P_{11}(x)$ and $C_{11}(y)$ are given by

$$P_{11}(x) = \frac{1}{\pi x^{\frac{1}{2}} (1 - x)^{\frac{1}{2}}}$$

$$C_{11}(y) = \frac{2}{\pi} \sin^{-1} (y^{\frac{1}{2}})$$

For M = 1, values of $P_{N1}(x), 2 \leq N \leq 16$, have been derived from $P_{11}(x)$ by iterative application of an approximate algorithm which was designed to calculate joint probability density functions. A description of this algorithm and details of its expected accuracy are given in the Appendix.

For values of M other than M = 1, and M = ∞, values of $P_{NM}(x), 1 \leq N \leq 16$, have been derived solely by digital simulation on a PDP 11/40 minicomputer. For each combination of N and M such that $1 \leq N \leq 16$, and M = 1, 2, 4, 8 or 16, 100,000 values of the estimate $g_{NM}(x)$ have been calculated for the assessment of confidence levels. The derivation of $P_{N1}(x), 1 \leq N \leq 16$, by digital simulation acts as a cross-check on the accuracy of the iterative calculation algorithm described in the Appendix and on the convergence of the digital simulation process.

For M = ∞, the amplitude of p(x) must, by the central limit theorem be normally distributed. The implication of this is that $g_{N\infty}(x)$ must be chi-squared distributed with N degrees of freedom, thus enabling values of $L_{N\infty}(\alpha)$ to be derived analytically from that distribution.

2.2 Numerical Results

The normalised values of $P_{N1}(x)$ and values of $C_{N1}(x)$ for $1 \leq N \leq 16$ are shown in Figures 1 and 2 respectively. As N increases $g_{N1}(x)$ tends to a normally distributed variable as predicted by the central limit theorem. In Figures 3, 4 and 5, values of $L_{NM}(\alpha)$ are shown for N and M

such that $1 \leqslant N \leqslant 16$ and M = 1, 2, 4, 8, 16 or ∞. The values of α correspond to tolerance bounds defined by $G_M(x)$ $\pm$1dB, $G_M(x)$ $\pm$2dB and $G_M(x)$ $\pm$3dB.

From Figures 3, 4 and 5 it can be seen that for given M and α, $L_{NM}(\alpha)$ increases monotonically with N. In addition, for given α and N (N>1) it can be seen that $L_{NM}(\alpha)$ decreases monotonically as M increases. This second conclusion is important since in many practical situations the value of M will not be known explicitly. In these circumstances however, it will be possible to state the upper and lower bounds of the confidence level that may be applied to any estimate $g_{NM}(x)$, (N>1) since for given N and α these are defined respectively by $L_{N1}(\alpha)$ and $L_{N\infty}(\alpha)$.

In particular, if $G_M(x)$ $\pm$3dB can be accepted as a tolerance band, then by squaring and averaging sixteen samples taken at random from any known or unknown one-dimensional distribution, the likelihood that the average is an accurate estimator of the true mean square of the distribution will lie between 94% and 100%.

Clearly, one conclusion that must be drawn is that a far better estimate of the mean power contained in a spatial measurement environment may be obtained by power averaging data derived at a relatively small number of locations than may be derived from a single measurement.

3. THE EFFECTS OF GAUSSIAN RANDOM NOISE ON ESTIMATES OF MEAN POWER FOR A SINGLE SINE WAVE

For a single pure sine wave contaminated by Gaussian random noise p(x) may be defined by

$$p(x) = \sin(kx) + n(x)$$

where n(x) is the instantaneous level of noise at x.

Since M = 1, $G_1(x)$, the mean power contained in the pure signal is given by

$$G_1(x) = \tfrac{1}{2}$$

$g_{N1}(x)$, the estimate of $G_1(x)$ is defined as

$$g_{N1}(x) = \frac{1}{N} \sum_{n=1}^{N} p^2(x_n)$$

where the x_n are N random values of x.

In these circumstances, it is necessary to define the signal to noise ratio SN as

$$SN = 20\log_{10} \left(\frac{\text{rms value of the signal}}{\text{rms value of the noise}} \right)$$

If the noise is assumed to be Gaussian random, then SN is related to the variance σ^2 by

$$\sigma^2 = \tfrac{1}{2}\, 10^{-SN/10}$$

for a unit amplitude sinusoidal signal.

Thus, for example, a signal to noise ratio of 0dB may be simulated by contaminating the pure unit amplitude sinusoidal signal with Gaussian random noise of zero mean and variance of 0.5.

The effects of noise on values of $L_{N1}(\alpha)$ have been calculated by digital simulation for values of SN ranging from 0dB to 40dB. The values of $L_{N1}(\alpha)$ already shown in Figures 3, 4 and 5 apply effectively to an infinite signal to noise ratio. For each combination of N and SN, 100,000 values of the estimate $g_{N1}(x)$ have been calculated in assessing the noise affected confidence levels.

Figures 6, 7 and 8 show the confidence levels $L_{N1}(\alpha)$ that the estimate $g_{N1}(x)$ lies within the tolerance bands $G_1(x)\pm 1$dB, $G_1(x)\pm 2$dB and $G_1(x)\pm 3$dB for values of SN equal to 0, 10, 20, 30, 40 and ∞.

As might be expected, the introduction of increasing levels of Gaussian random noise into the pure sinusoidal signal causes a monotonic reduction in confidence levels, although this degradation is insignificant for signal to noise ratios in excess of 20dB.

4. APPLICATION TO ACOUSTIC NOISE MEASUREMENT IN SHALLOW WATER

The apparent acoustic source radiation measured at a point in a bounded medium is invariably composed of the phased contributions from many interfering propagation paths which result from reflections at the boundaries of the medium. In this context, shallow water may be defined as a bounded medium in which the effects of multipath propagation are significant at any required measurement point.

In the idealised case of a fluid layer bounded by a free surface, $z = h$ and a hard surface $z = o$, the far field acoustic radiated pressure due to an omnidirectional point source situated at $(0, z_o)$ may be expressed at radian frequency w by a normal mode expansion as shown in Reference 1. Thus,

$$p(r,z,t) = \frac{2iw\varrho}{h} \exp\left(\frac{i\pi}{4}\right)\left(\frac{2\pi}{r}\right)^{\frac{1}{2}} \sum_{L=1}^{\infty} \cos(b_L z_o)\cos(b_L z).\ \xi_L^{-\frac{1}{2}}.\exp(i\xi_L r)\exp(iwt) \qquad (4.1)$$

where $b_L = \frac{(L-\frac{1}{2})\pi}{h}$

and $h\xi_L = \left[(kh)^2 - (L-\frac{1}{2})^2\pi^2\right]^{\frac{1}{2}}$ $\quad L = 1, 2 \ldots.$

(r, θ, z) are cylindrical coordinates as defined in Figure 10.

It is convenient to define a mode number M such that ξ_M is real and ξ_{M+1} is imaginary. It is then important to note that modes defined by mode number $L \leq M$ propagate efficiently to the far-field whereas modes defined by $L > M$ attenuate exponentially away from the source. Under conditions in which ξ_1 is imaginary, all of the normal modes attenuate exponentially away from the source. In addition for $L \leq M$ the power propagated by the efficient normal modes increases monotonically with mode number L. Thus, the far-field acoustic pressure may be expressed by the sum of the pressures contributed by M normal modes each of which has sinusoidal depth dependence.

In general, it is required that measurements of the far-field acoustic pressure generated in shallow water by a directional source should yield the mean power that is propagating through the cylindrical sector defined by $r = r_o$ = constant and $\theta_o - \delta \leq \theta \leq \theta_o + \delta$ where δ is a function of the source directivity.

In sea water, suitable measurements may be made by a vertical array of randomly spaced transducers which are located at the positions (r_o, θ_o, z_i), r_o and θ_o being constant.

For an omnidirectional source, situated in an ideal cylindrical channel, the far field acoustic pressure measured at radian frequency w by the ith element of such an array is defined by (4.1) which for constant r and θ may be simplified to give

$$p(z_i,t) = \sum_{L=1}^{M} a_L(r_o) \cos(b_L z_i) \exp(iwt)$$

The power spectrum of the time variation of $p(z_i,t)$ may be defined by its amplitude $s(z_i)$ which is given by

$$s(z_i) = \sum_{L=1}^{M} a_L(r_o) \cos(b_L z_i)$$

If the true mean power propagating through the cylindrical sector $r = r_o$, $\theta_o - \delta \leq \theta \leq \theta_o + \delta$ is given by $G_M(z)$ then an estimate of $G_M(z)$ may be defined as $h_{NM}(z)$ where

$$h_{NM}(z) = \frac{1}{N} \sum_{n=1}^{N} s^2(z_n)$$

the z_n being randomly selected values of z.

$h_{NM}(z)$ is related to $G_M(z)$ by the expression

$$G_M(z) = \lim_{N \to \infty} h_{NM}(z)$$

Although the estimates $h_{NM}(z)$ and $g_{NM}(x)$ have identical forms, the confidence levels $L_{NM}(\alpha)$ which apply to the estimates $g_{NM}(x)$ may not strictly be applied to the estimates $h_{NM}(z)$ since s(z) is synthesised by harmonically related sinusoids of unequal amplitude. However, it will be demonstrated that the confidence levels $L_{N1}(\alpha)$ and $L_{N\infty}(\alpha)$ may be considered as upper and lower bounds for the confidence levels which apply to values of $h_{NM}(z)$.

In order to assess the applicability of $L_{NM}(\alpha)$ to estimates $h_{NM}(z)$, a further digital simulation has been carried out to derive the confidence levels $T_{NM}(\alpha)$ which may be applied to the estimates $h_{NM}(z)$ for the particular measurement geometry in which a horizontal range of 100m exists between the measuring array and a source situated at mid-depth in water 61m deep. For this horizontal

range, the exponentially decaying modes will still contribute significantly to the measured radiation in the frequency range 0-30Hz which is equivalent to values of $M \leq 2$. The application of the confidence levels $T_{N1}(\alpha)$ and $T_{N2}(\alpha)$ to measurements using this geometry will thus be erroneous in practice. However, the quantity $T_{NM}(\alpha) - L_{NM}(\alpha)$ will give a good measure of the effects on confidence levels of non-uniform normal mode amplitudes and of harmonic relationships between the individual propagating normal modes.

In the derivation of $T_{NM}(\alpha)$ each value of M effectively defines a frequency range in which exactly M propagating normal modes exist. For each M, this frequency range has been split into ten thousand bands, and at each band centre frequency f_o an estimate $h_{NM}(z)$ has been formed by averaging the squared pressures calculated from (4.1) at N randomly generated depths. The confidence levels $T_{NM}(\alpha)$ have been derived by comparing each value of $h_{NM}(z)$ with the respective true mean square pressure propagating at the frequency f_o. For each combination of N and M, only 10,000 values of $h_{NM}(z)$ have been computed due to the time consuming nature of the calculation described by (4.1).

Values of $T_{NM}(\alpha)$ are presented implicitly in Figure 9 which gives values of $T_{NM}(\alpha) - L_{NM}(\alpha)$. Since $T_{N1}(\alpha)$ and $L_{N1}(\alpha)$ should be identical for given N and α, the slight deviations of $T_{N1}(\alpha) - L_{N1}(\alpha)$ from zero give a measure of the inaccuracies introduced by the digital simulation processes.

From Figure 9, it is apparent for $N>3$ that $T_{NM}(\alpha) - L_{NM}(\alpha)$ is strictly positive for $M>1$. For other combinations of N and M, the quantity $T_{NM}(\alpha) - L_{NM}(\alpha)$ is generally positive except in a few isolated cases in which the negative excursions are within the bounds that might be expected to result from inaccuracies inherent to the digital simulation procedures. It may also be deduced from Figure 9 that for $N>3$, $T_{NM}(\alpha)$ is always bounded by the confidence levels $L_{N1}(\alpha)$ and $L_{N\infty}(\alpha)$. Thus

$$L_{N\infty}(\alpha) \leq T_{NM}(\alpha) \leq L_{N1}(\alpha) \qquad (N>3,\ 1 \leq M \leq \infty)$$

This is an extremely important conclusion, since it implies that $L_{N1}(\alpha)$ and $L_{N\infty}(\alpha)$ act as bounds for the confidence levels that apply to estimates of mean radiated power that have been derived in shallow water by power averaging the frequency domain outputs of randomly spaced elements that form a vertical array.

For an array of 12 randomly spaced elements, the level of confidence that the power average of the individual array element outputs is within ±3dB of the true mean radiated power lies between 89.5% and 99.5%. The equivalent confidence bounds for an array of 16 elements are 94% and 100%.

4.1 Experimental results of noise propagation trials, undertaken in shallow water

In February 1975, AMTE carried out a series of noise propagation trials in shallow water in which the noise radiated by a hydrosounder at a horizontal range of 100m was measured by a vertical five element hydrophone array. The hydrosounder, which is practically omnidirectional in the frequency range 0 - 1kHz, was situated at a depth of 30m in water of depth 80m. A single hydrophone was situated 10m directly above the hydrosounder in order to monitor the source output. This monitor hydrophone may be considered as being in the acoustic far-field of the source at frequencies above 300Hz. The layout of the experimental facility is shown in Figure 10.

Experimental data gained from these trials are shown in Figures 11, 12 and 14. All of these data have been analysed using Fast Fourier Transform techniques as implemented in Reference 3.

Figure 11 shows the frequency power spectrum of the monitor hydrophone response to a hydrosounder output of the form of shaped band limited random noise in the frequency band 250Hz - 1kHz. The nominal bandwidth is 4Hz. The response is not completely smooth due to the interfering effects of the first surface reflection. From Figure 12, which shows the transfer functions between each array element and the monitor hydrophone, it is clear that the measured radiated pressure may be described accurately by the contributions from only two propagation paths. These are the direct path and the path which embodies a single surface reflection. On this assumption of radiation into a half space, calculated theoretical predictions of the data shown in Figure 12 are shown for comparison in Figure 13. The agreement is remarkably good for the array elements situated at depths of 24, 30 and 38 metres, but for the elements at 47m and 56m, the effects of reflections from the sea bed cause some deterioration in the detail agreement.

As was shown earlier in this section, a good estimate of the mean power radiated by the hydrosounder at a range of 100m may be obtained by averaging the power spectra derived from the individual array elements. However, if the narrow band radiated pressure is to be related to a known excitation, 3dB must be added to the spatial average of the transfer function between the array elements and the excitation, which is defined by the monitor hydrophone. This is because the narrow band source spectrum will always describe the peak square value of the excitation in each narrow frequency band. Since the spatially averaged narrow band transfer function should relate the mean square radiated pressure to the mean square level of the excitation, 3dB should be added to the averaged transfer function in order to convert the peak square level of the excitation to its more appropriate mean square level.

Figure 14 shows the result of adding 3dB to the power average of the experimental transfer functions shown in Figure 12. The data in Figure 14(a) have been likewise derived from the theoretical data presented in Figure 13. The major conclusion that may be drawn from these Figures is that the power averaging of even a small number of array element outputs leads to significant improvements in the accuracy of radiated noise transfer functions.

In the case of acoustic radiation by a point source into a half space, $p(z)$, the variation of pressure with depth (z) at a fixed horizontal range r_o, is not explicitly sinusoidal. However for practical measurements, $p(z)$ may either be expanded into a discrete harmonic series or into a continuous wavenumber spectrum. In either case, for a given number of array elements, N, and for a given tolerance band α, a lower bound given by $L_{N\infty}(\alpha)$ may be stated for the confidence levels that are applicable to a transfer function that has been derived by power averaging the N frequency power spectra of the individual array elements. Values of $L_{N\infty}(\alpha)$ may be derived from Figures 3, 4 or 5.

Figure 5 shows that the use of 5 array elements for estimating the mean propagating power implies that the likelihood of the estimate being within ±3dB of the true mean lies between 70% and 94%. This is borne out by Figure 14 which shows a scatter of ±4dB.

Figure 15 shows third octave transfer functions between the individual array elements and the monitor hydrophone. Figure 16 shows the results of adding 3dB to the power average of these transfer functions. These Figures also include theoretical losses for point source radiation into an infinite medium and into a half space. From these Figures, it is apparent that third octave smoothing is useful in removing the effects of propagation whenever the source spectrum is relatively flat. It must be stressed however that for other source characteristics, third octave averaging is not suitable for removing the effects of multi-path propagation.

From Figure 16, it is also clear that the addition of 3dB to the averaged transfer function provides a suitable estimate of the mean power propagating away from the source at a range of 100m since the propagation loss between the source and the array is, as might be expected of radiation into a half space, about 3dB less than the equivalent free-field propagation loss.

5. CONCLUSIONS

Confidence levels $L_{NM}(\alpha)$ applicable to $g_{NM}(x)$ have been derived where $g_{NM}(x)$ is an estimate of the mean power contained in $p(x)$, the sum of M sinusoids of equal amplitude and random argument. $g_{NM}(x)$ and $p(x)$ are defined by

$$p(x) = \sum_{m=1}^{M} \sin\phi_m$$

$$g_{NM}(x) = \frac{1}{N} \sum_{n=1}^{N} p^2(x_n)$$

where ϕ_m and x_n are random variables with even distributions.

$L_{NM}(\alpha)$ is defined as the level of confidence that any estimate $g_{NM}(x)$ lies within $10\log_{10}\alpha$dB of the true mean square value of $p(x)$ which is given by $\frac{1}{2}M$.

It has also been shown that $L_{N1}(\alpha)$ and $L_{N\infty}(\alpha)$ act as bounds for the confidence levels which apply whenever the sinusoids that synthesise p(x) have unequal amplitudes and are harmonically related. This enables the $L_{NM}(\alpha)$ to be applied to measurements of acoustic radiated noise taken in bounded media. In this context, it has been shown, both theoretically and experimentally, that significant improvements in estimates of the mean radiated power propagating in shallow water may be achieved by power averaging the frequency spectra obtained from the individual randomly spaced elements of a vertical array. It is concluded that the use of 12 elements in this way leads to an estimate that is between 90% and 99% certain of being within ±3dB of the true mean radiated power. Moreover, the confidence levels $L_{N\infty}(\alpha)$ represent lower bounds of the confidence levels that may be applied to estimates $g_{N\infty}(x)$ where measurements are taken of any type of signal variation.

A W Walker

AWW/APG

REFERENCES

1. BREKHOVSKIKH, L.M., Waves in Layered Media, Academic Press 1960.

2. PANTER, R.J. et al, Unpublished data resulting from Underwater Propagation Trials (AMTE) February 1975.

3. WALKER, A.W., A PDP Computer Software General Purpose Spectrum Analyser and its Application to the Analysis of Data Resulting from Vibration Testing, ARL/N/N3 1977.

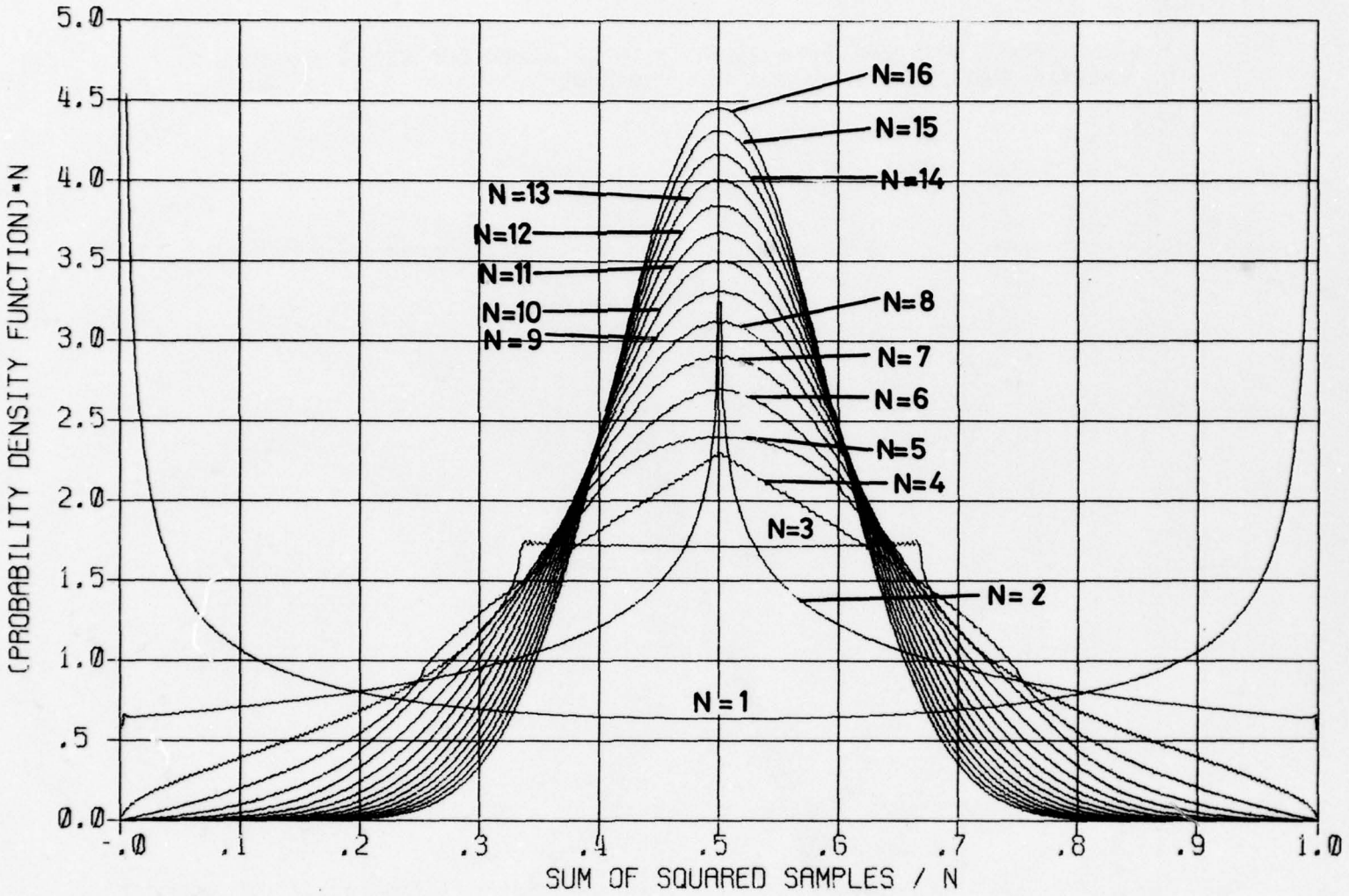

FIG. 1 NORMALISED PROBABILITY DENSITY FUNCTIONS FOR THE AVERAGE OF THE SQUARES OF N SAMPLES TAKEN RANDOMLY FROM A SINGLE PURE SINE WAVE, $1 \leq N \leq 16$

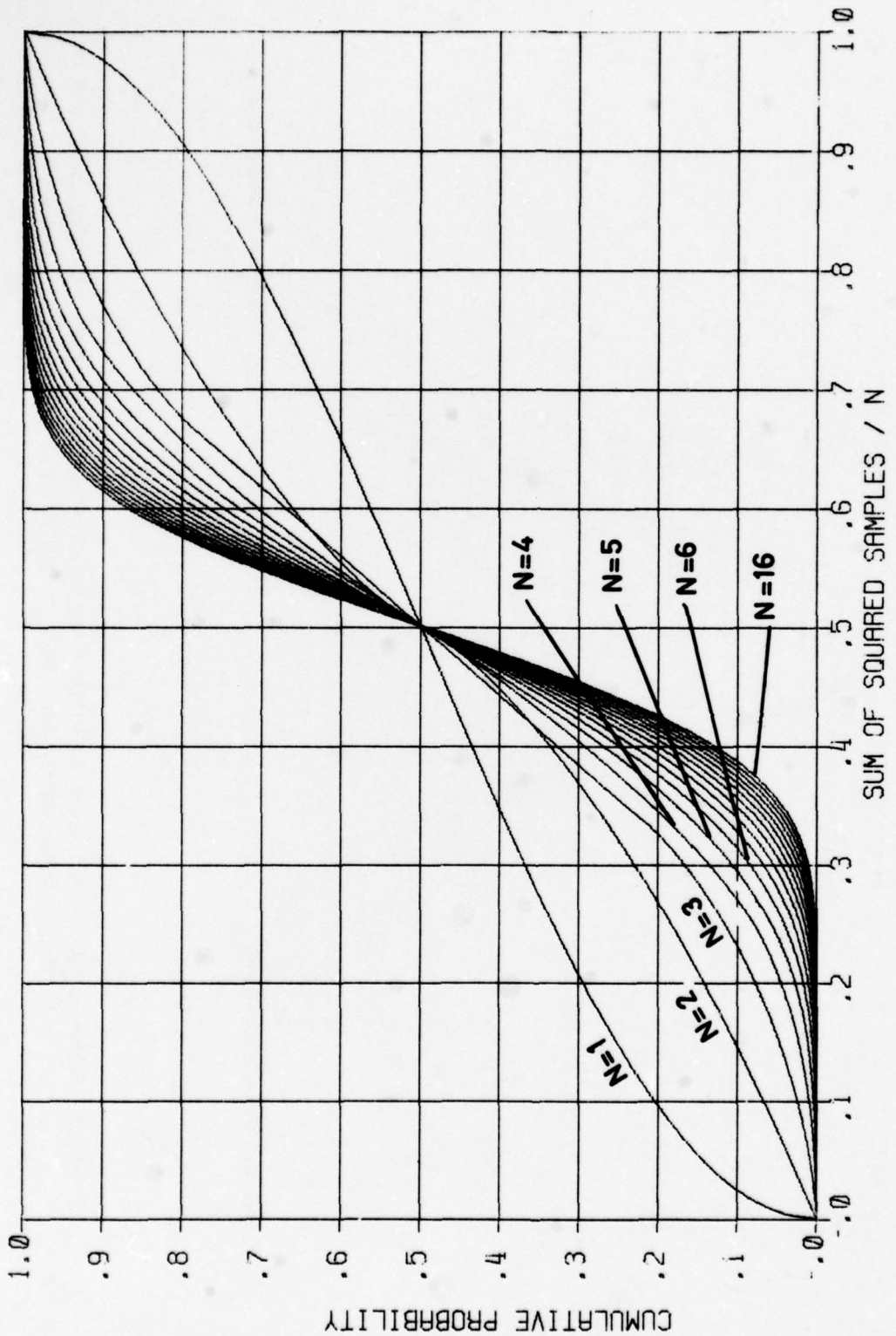

FIG. 2 CUMULATIVE PROBABILITY FUNCTIONS FOR THE AVERAGE OF THE SQUARES OF N SAMPLES TAKEN RANDOMLY FROM A SINGLE PURE SINE WAVE, $1 \leq N \leq 16$

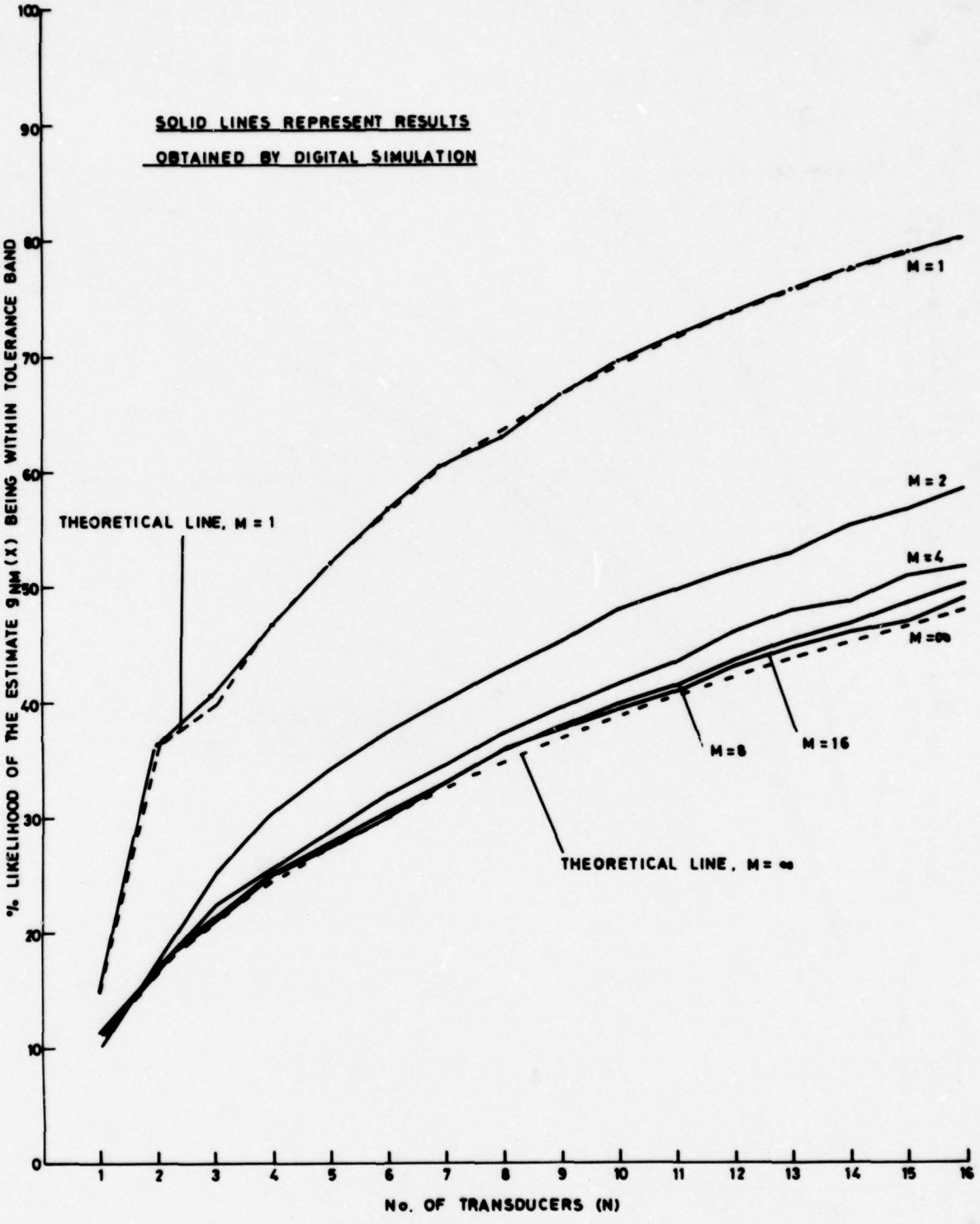

FIG. 3 CONFIDENCE LEVELS $L_{NM}(\infty)$ THAT THE ESTIMATE $g_{NM}(X)$ IS WITHIN ±1dB OF THE TRUE SIGNAL MEAN SQUARE VALUE WHEN N SAMPLES ARE TAKEN RANDOMLY FROM THE SUM OF M PURE SINE WAVES OF EQUAL AMPLITUDE AND RANDOM WAVENUMBER

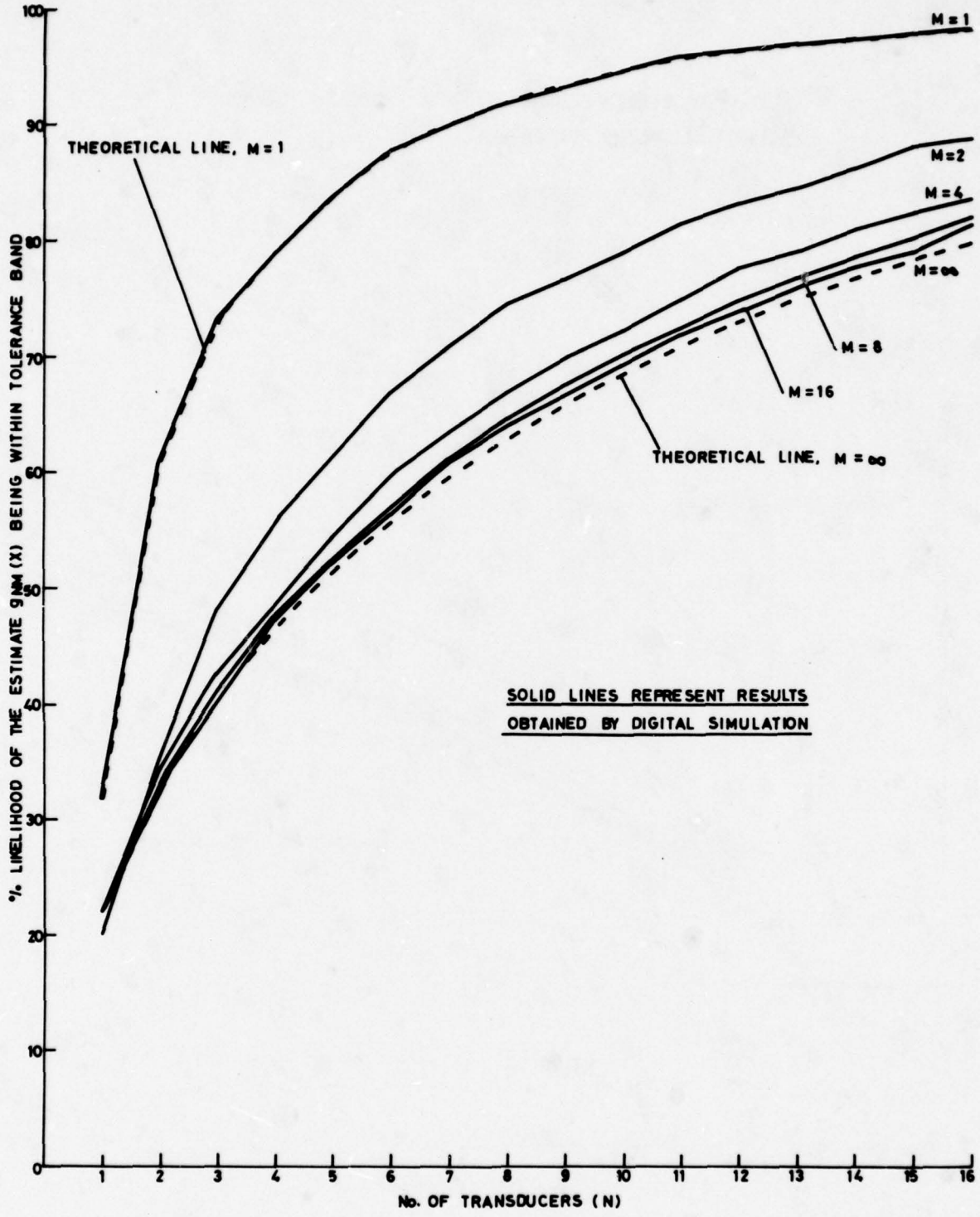

FIG. 4 CONFIDENCE LEVELS $L_{NM}(\alpha)$ THAT THE ESTIMATE $g_{NM}(X)$ IS WITHIN ±2dB OF THE TRUE SIGNAL MEAN SQUARE VALUE WHEN N SAMPLES ARE TAKEN RANDOMLY FROM THE SUM OF M PURE SINE WAVES OF EQUAL AMPLITUDE AND RANDOM WAVENUMBER

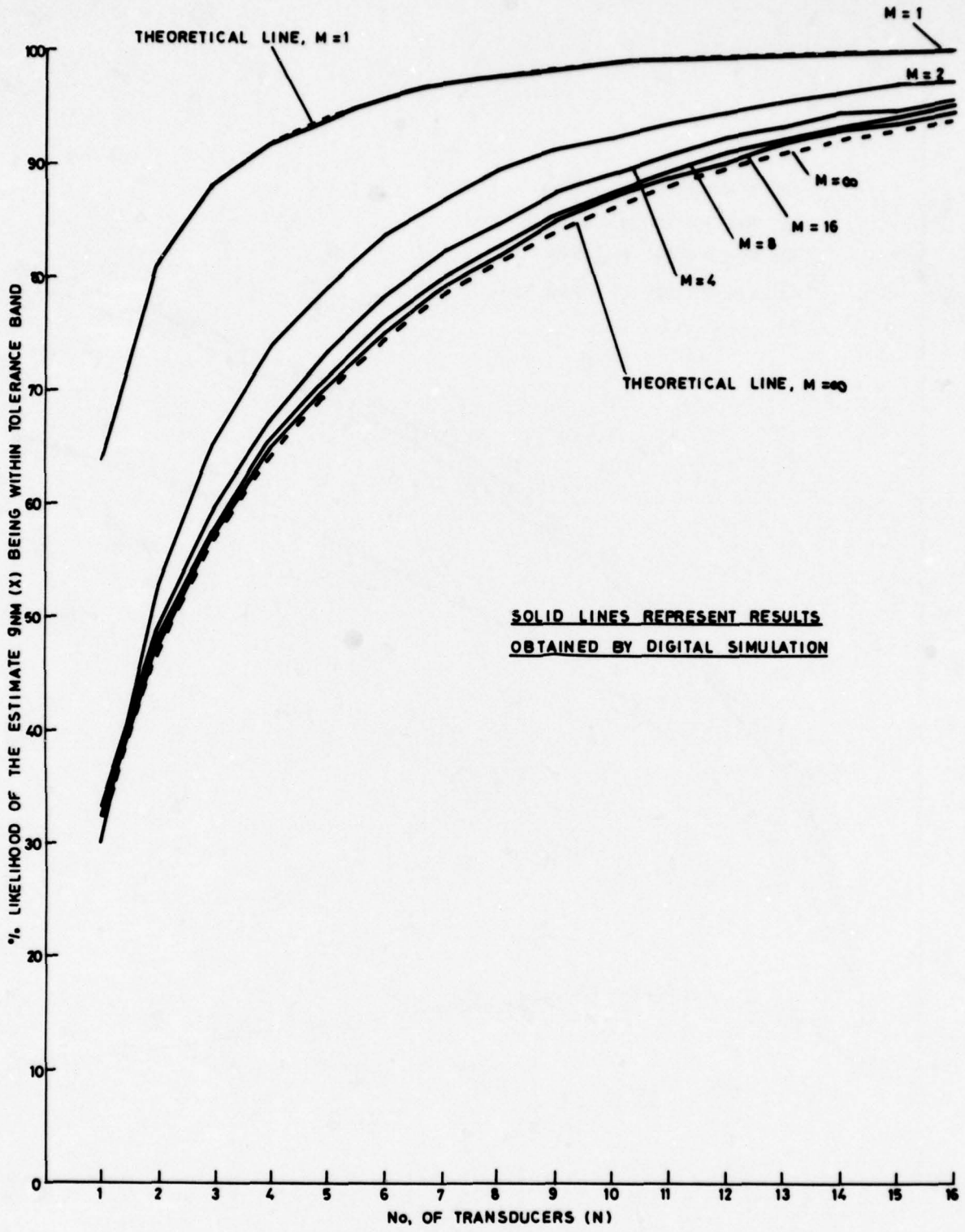

FIG. 5 CONFIDENCE LEVELS $L_{NM}(\alpha)$ THAT THE ESTIMATE $g_{NM}(X)$ IS WITHIN ±3dB OF THE TRUE SIGNAL MEAN SQUARE VALUE WHEN N SAMPLES ARE TAKEN RANDOMLY FROM THE SUM OF M PURE SINE WAVES OF EQUAL AMPLITUDE AND RANDOM WAVENUMBER

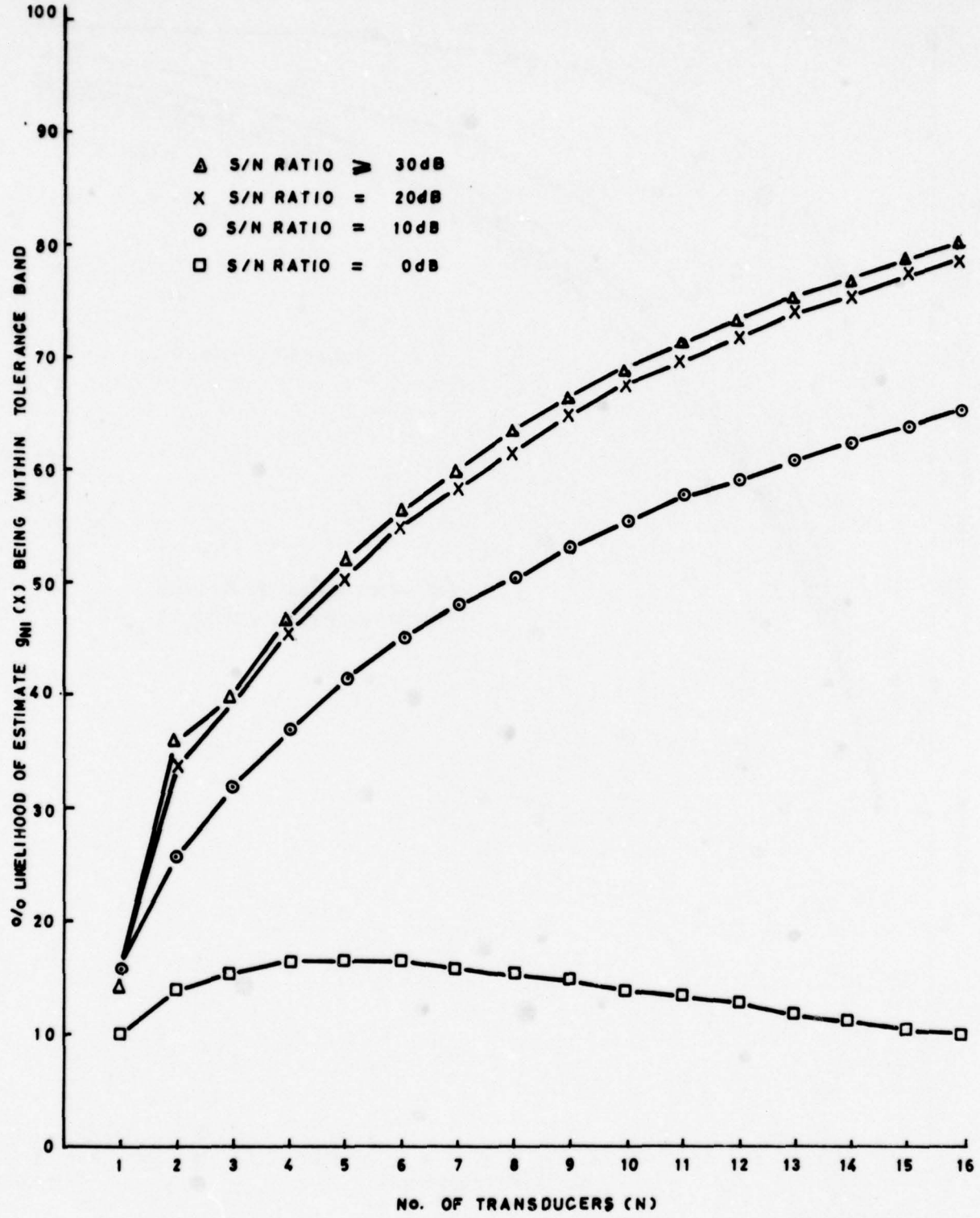

FIG. 6. CONFIDENCE LEVELS THAT THE ESTIMATE $g_{NI}(X)$ IS WITHIN ±1dB OF THE TRUE SIGNAL MEAN SQUARE VALUE WHEN N SAMPLES ARE TAKEN RANDOMLY FROM A SINGLE SINE WAVE CONTAMINATED BY VARYING LEVELS OF GAUSSIAN RANDOM NOISE

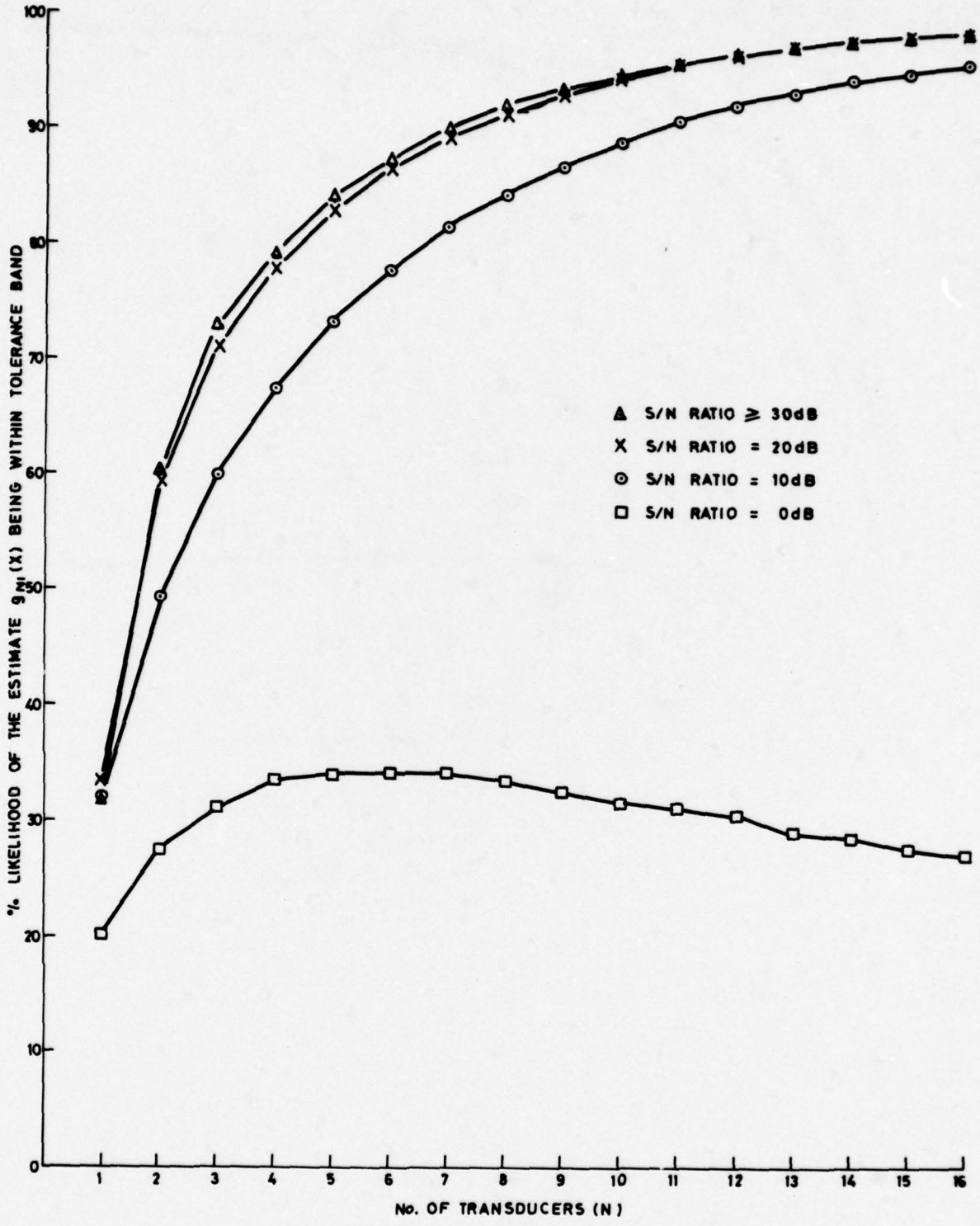

FIG. 7 CONFIDENCE LEVELS THAT THE ESTIMATE $g_{NI}(X)$ IS WITHIN ±2dB OF THE TRUE SIGNAL MEAN SQUARE VALUE WHEN N SAMPLES ARE TAKEN RANDOMLY FROM A SINGLE SINE WAVE CONTAMINATED BY VARYING LEVELS OF GAUSSIAN RANDOM NOISE

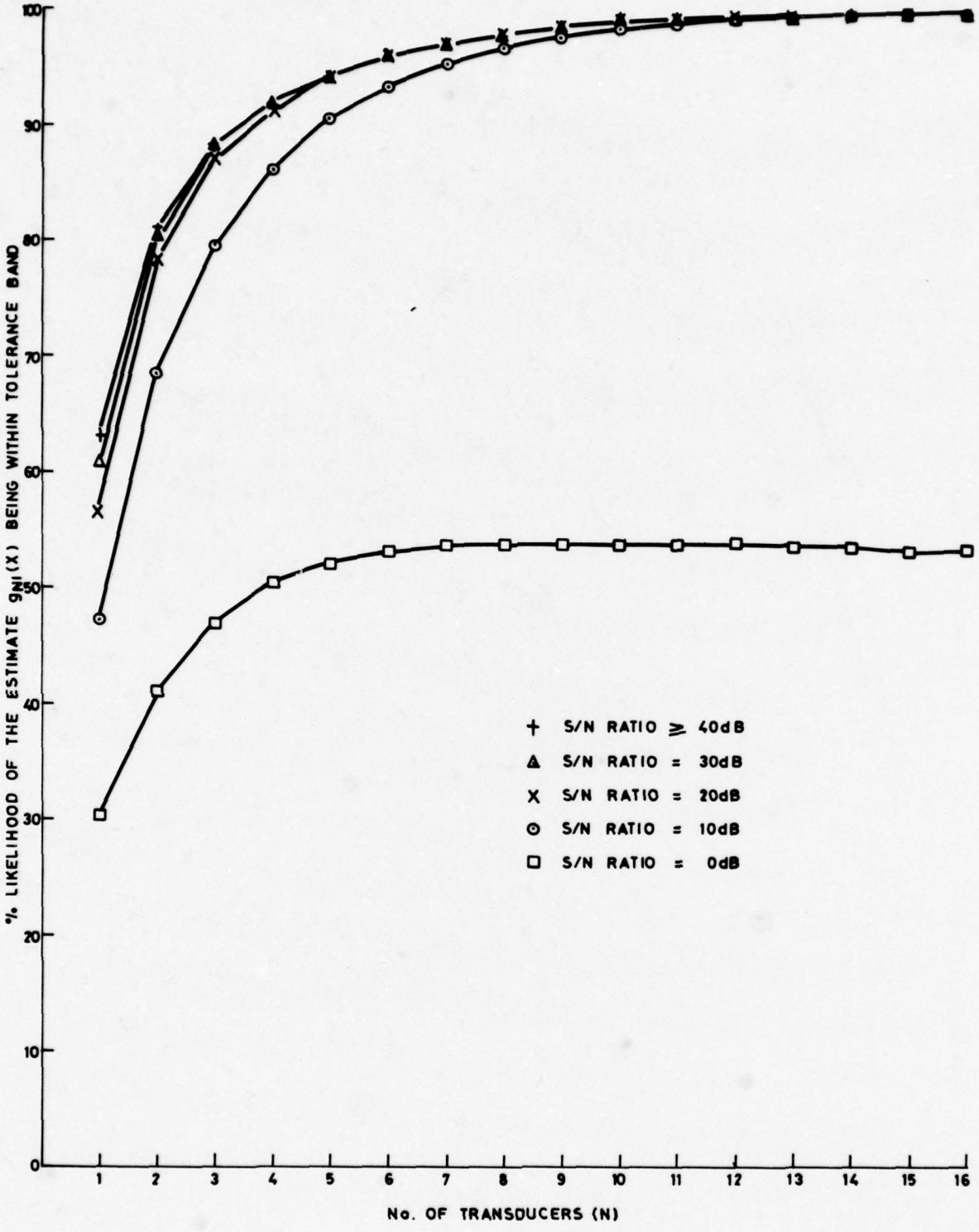

FIG. 8 CONFIDENCE LEVELS THAT THE ESTIMATE $g_{NI}(X)$ IS WITHIN ±3dB OF THE TRUE SIGNAL MEAN SQUARE VALUE WHEN N SAMPLES ARE TAKEN RANDOMLY FROM A SINGLE SINE WAVE CONTAMINATED BY VARYING LEVELS OF GAUSSIAN RANDOM NOISE

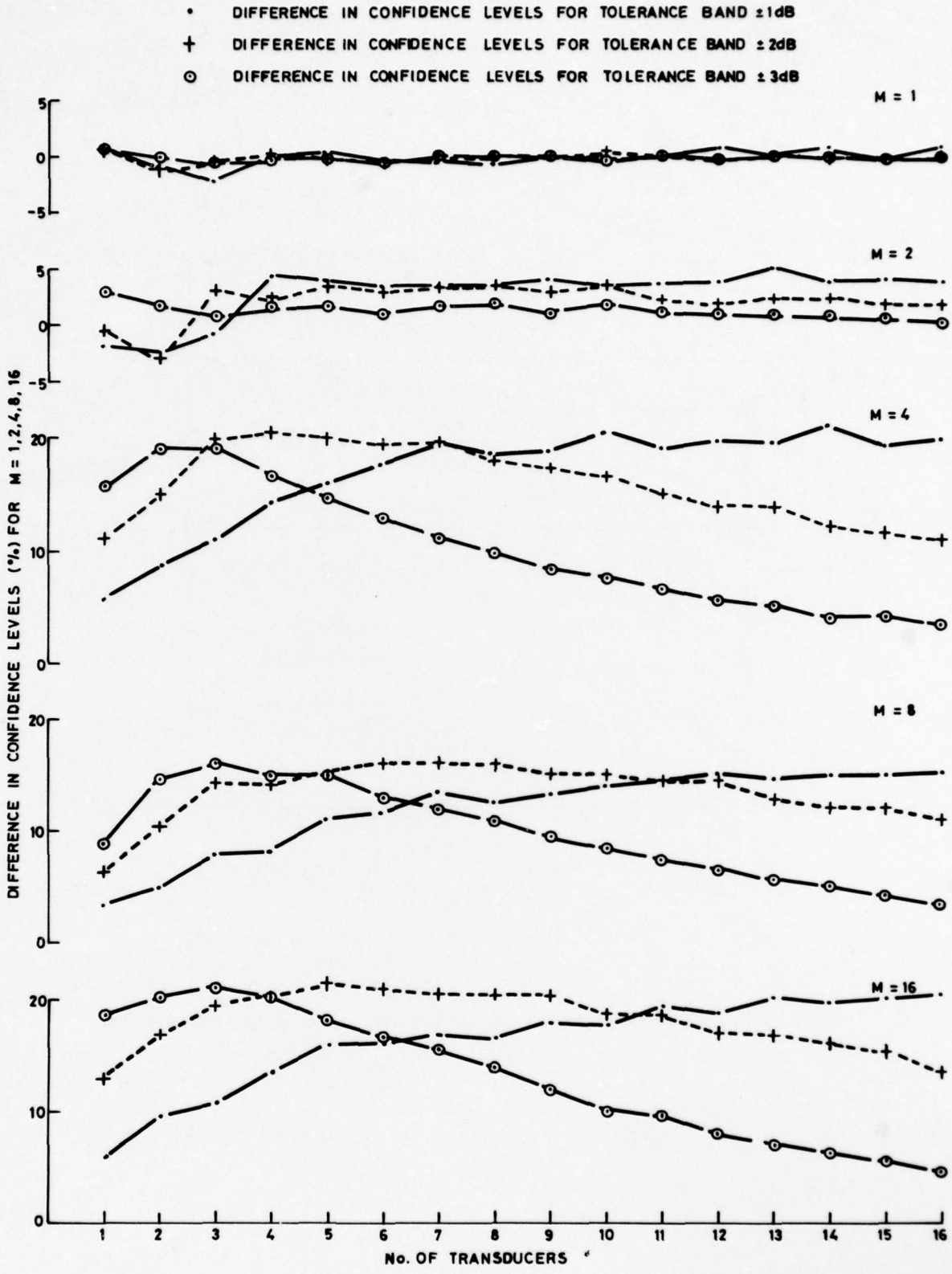

FIG. 9 DIFFERENCE IN CONFIDENCE LEVELS ($T_{NM}(\alpha) - L_{NM}(\alpha)$) FOR $1 \leq N \leq 16$, M = 1, 2, 4, 8 AND 16 AND FOR VALUES OF α EQUIVALENT TO TOLERANCE BANDS OF MEAN SQUARE ±1dB, ±2dB, ±3dB

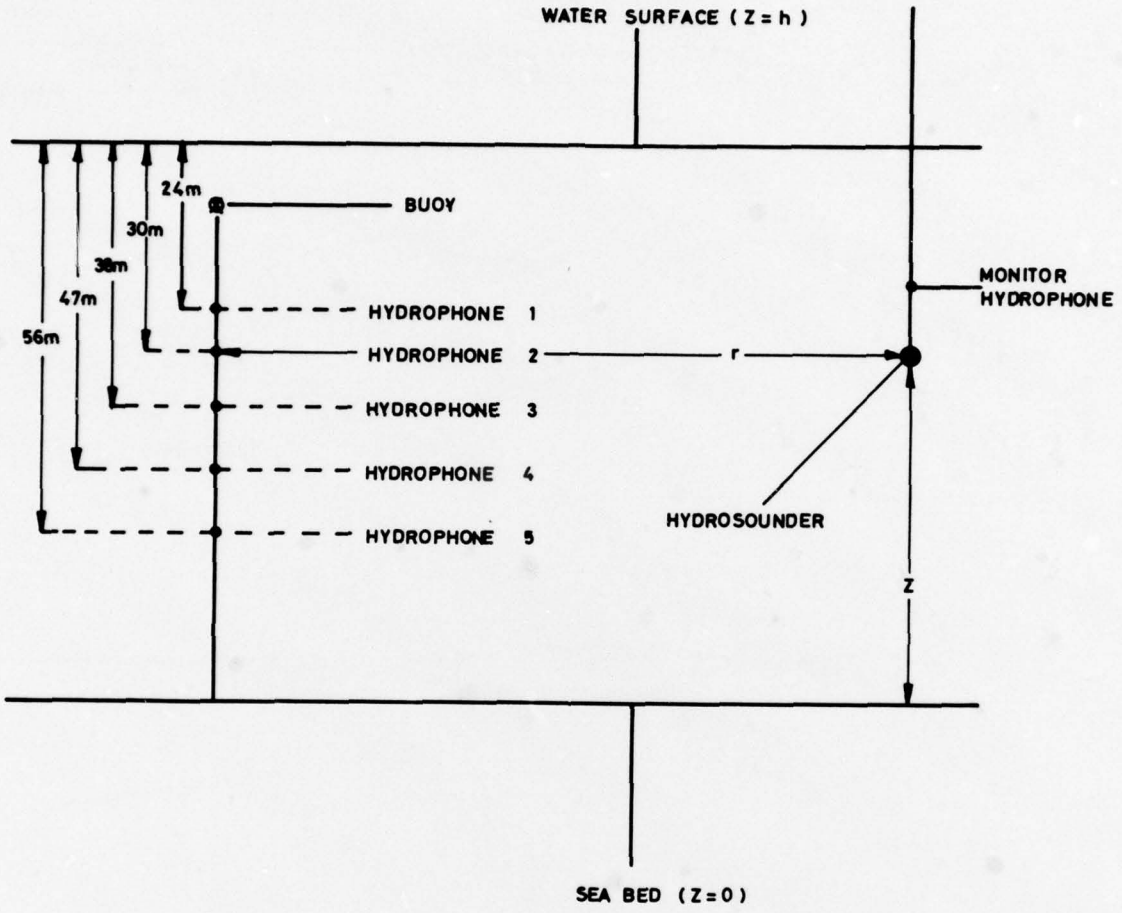

Θ IS THE ORIENTATION OF THE SOURCE IN A PLANE PARALLEL TO THE SURFACE

FIG. 10 SCHEMATIC LAYOUT OF EXPERIMENTAL FACILITY

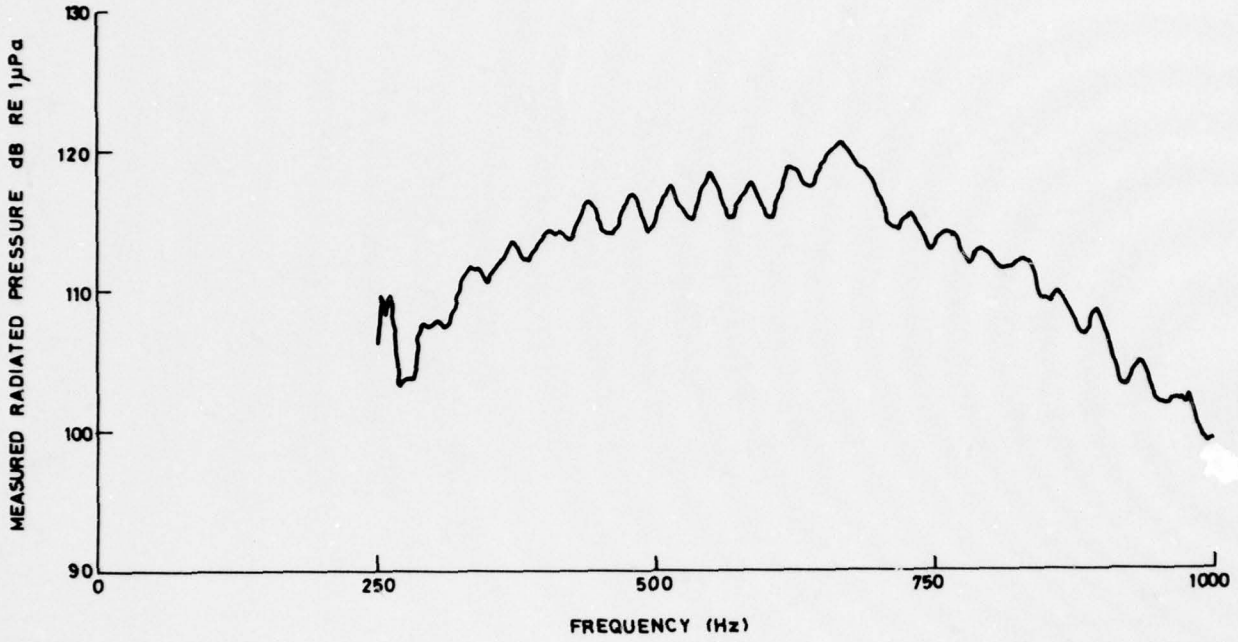

FIG 11 MONITOR HYDROPHONE RADIATED NOISE RESPONSE TO HYDROSOUNDER OUTPUT OF THE FORM OF BAND LIMITED RANDOM NOISE dB REF 1μPa

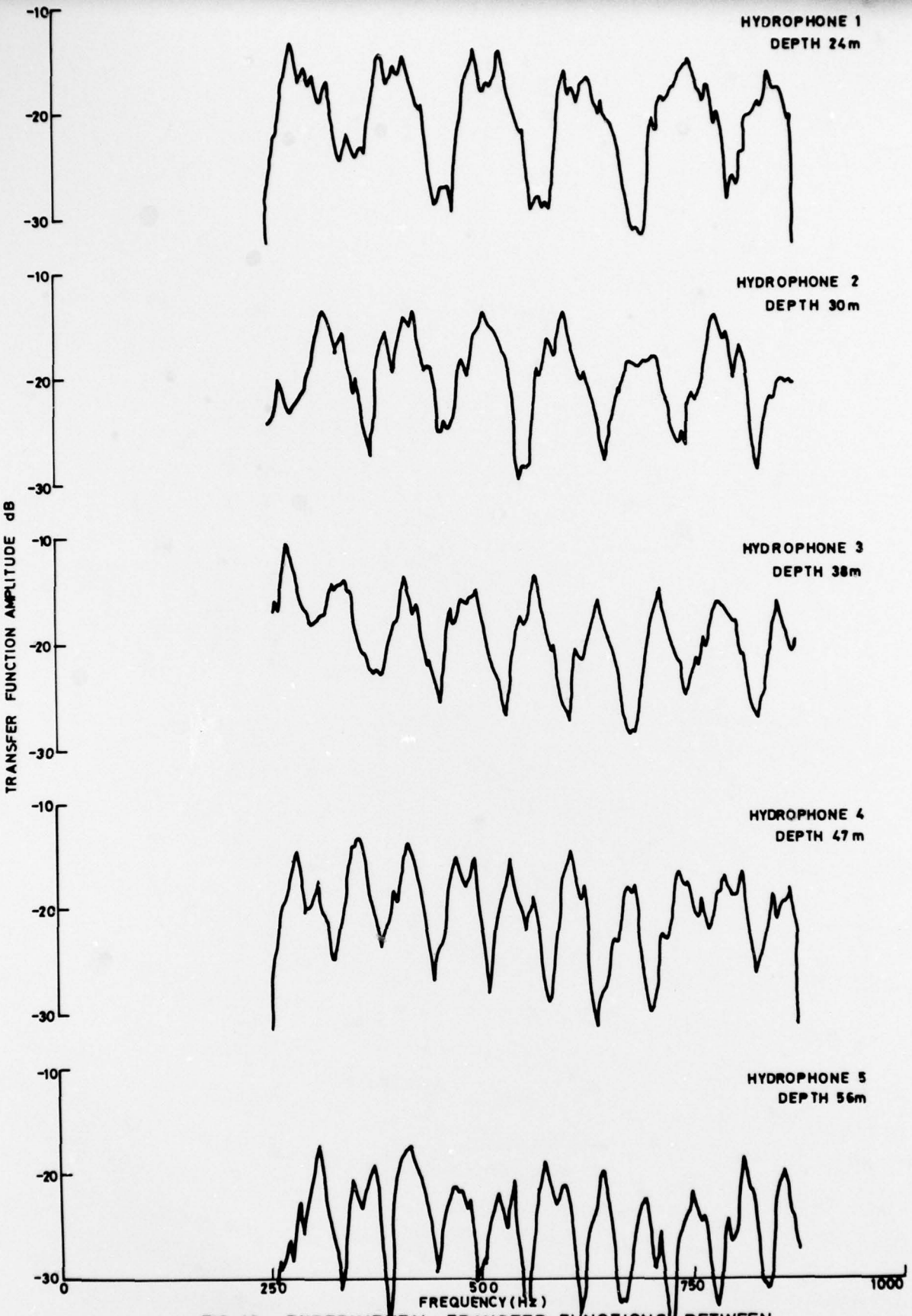

FIG. 12 EXPERIMENTAL TRANSFER FUNCTIONS BETWEEN INDIVIDUAL ARRAY ELEMENTS AND MONITOR HYDROPHONE

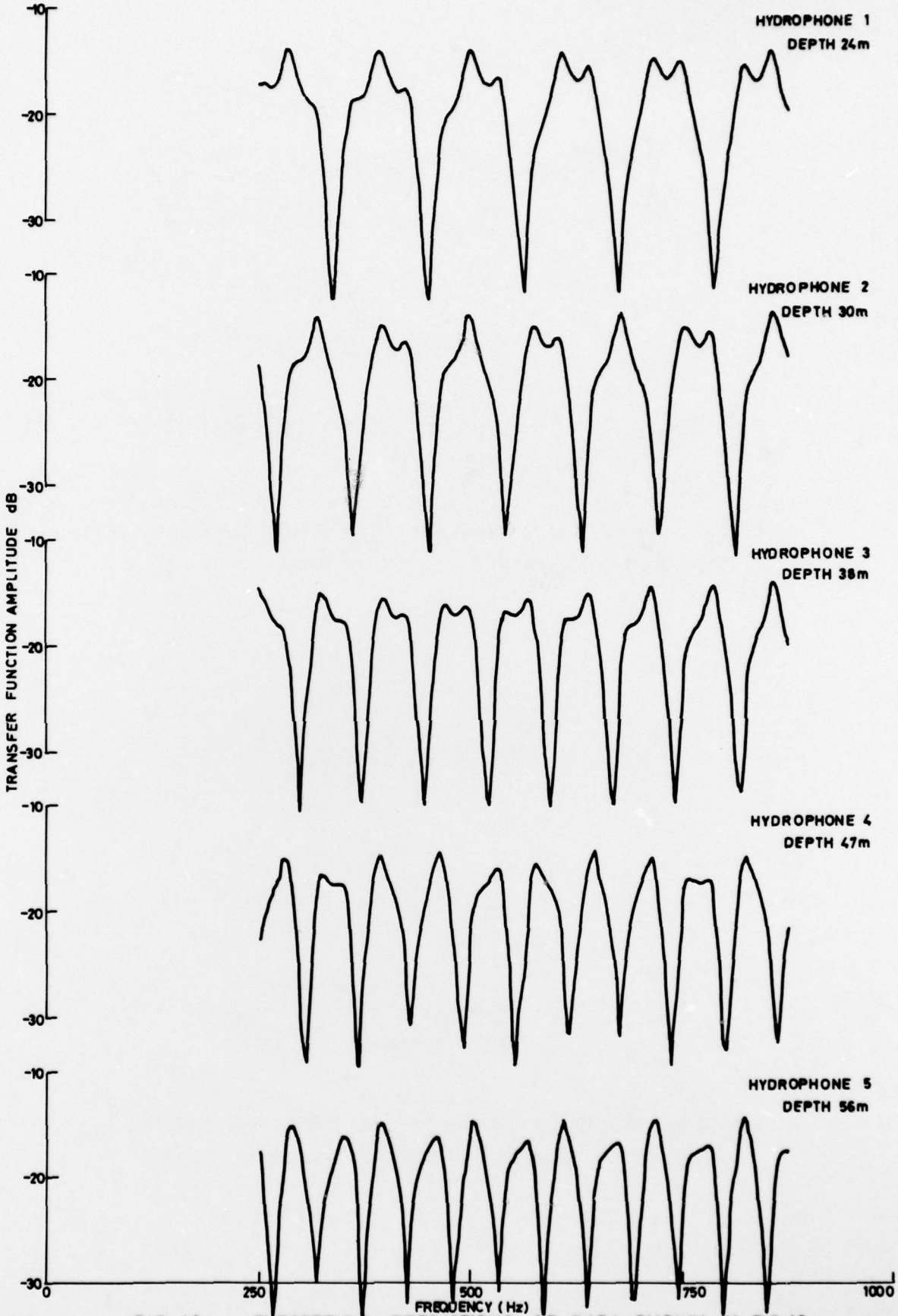

FIG. 13 THEORETICAL PREDICTIONS OF DATA SHOWN IN FIG. 12 ASSUMING POINT SOURCE RADIATION INTO A HALF-SPACE

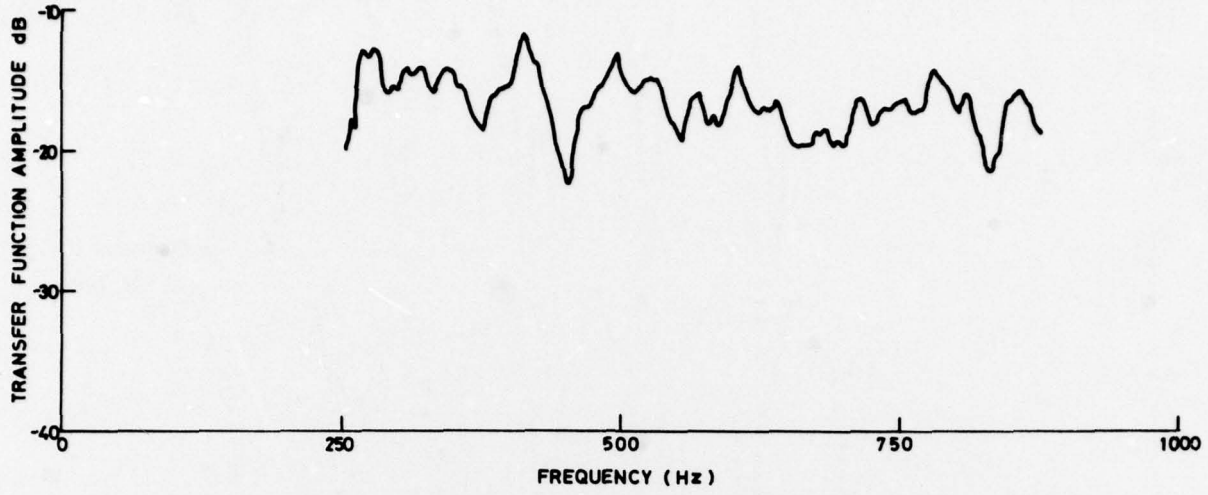

FIG. 14 RESULT OF ADDING 3dB TO POWER AVERAGE OF EXPERIMENTAL TRANSFER FUNCTIONS SHOWN IN FIG. 12

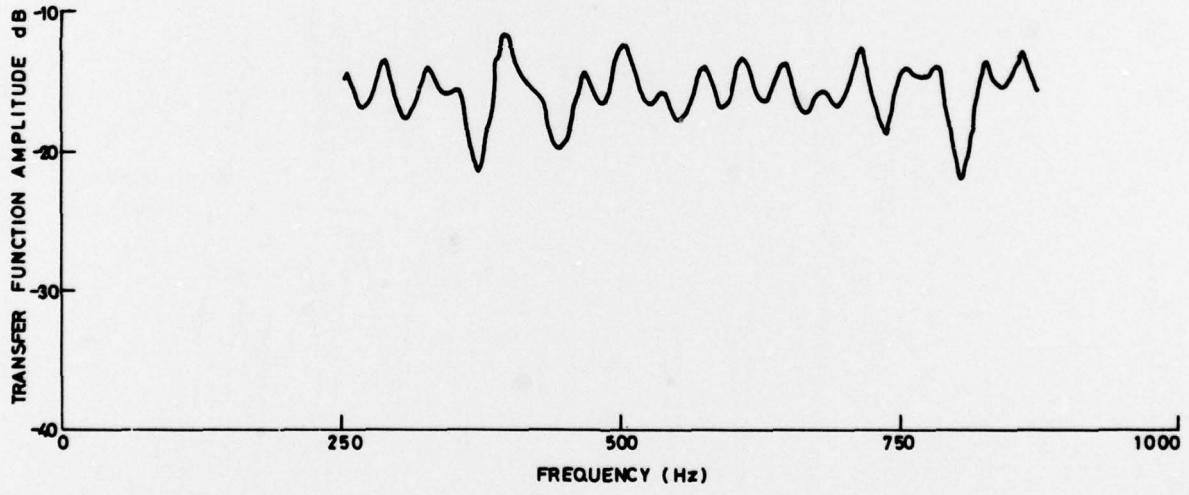

FIG. 14 (a) RESULT OF ADDING 3dB TO POWER AVERAGE OF THEORETICAL TRANSFER FUNCTIONS SHOWN IN FIG. 13

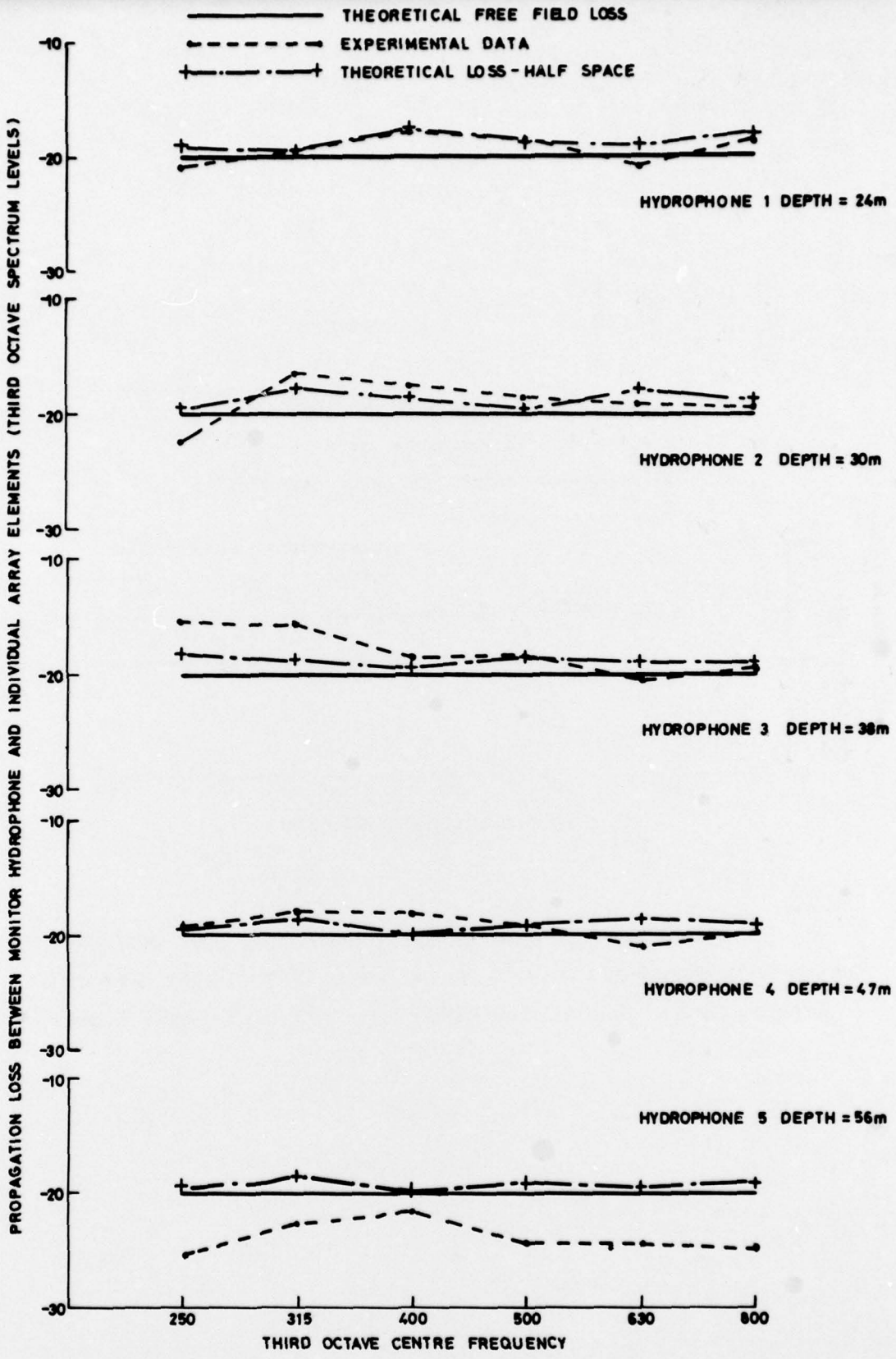

FIG. 15 EXPERIMENTAL THIRD OCTAVE PROPAGATION LOSSES BETWEEN MONITOR HYDROPHONE AND INDIVIDUAL ARRAY ELEMENTS COMPARED WITH EQUIVALENT THEORETICAL FREE-FIELD AND HALF-SPACE LOSSES

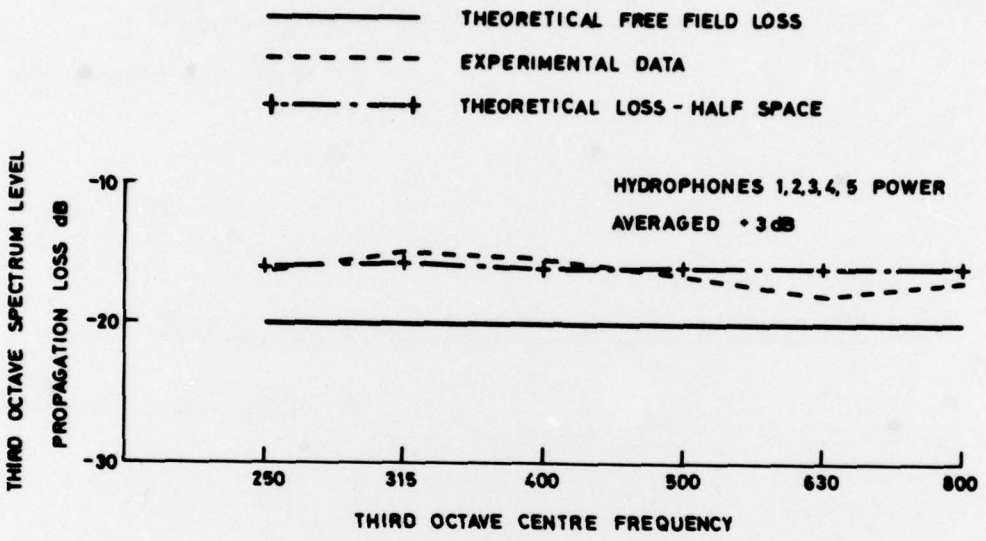

FIG. 16 EXPERIMENTAL THIRD OCTAVE PROPAGATION LOSS BETWEEN MONITOR HYDROPHONE AND POWER AVERAGED ARRAY OUTPUTS +3dB COMPARED WITH EQUIVALENT THEORETICAL FREE-FIELD AND HALF-SPACE LOSSES

APPENDIX

CALCULATION ALGORITHM FOR DETERMINATION OF JOINT PROBABILITY DENSITY FUNCTIONS

The calculation algorithm described in this Appendix has been developed specifically to allow $P_{N1}(x)$ to be derived by iterative means from $P_{11}(x)$ as the sole input.

Strictly $P_{N1}(x)$ should be derived from $P_{11}(x)$ alone by evaluation of the expression

$$P_{N1}(y) = \iint \cdots \int_{x_1 + x_2 + \cdots + x_N = y} P_{11}(x_1)P_{11}(x_2)\cdots P_{11}(x_N)dx_1dx_2\cdots dx_N$$

Numerical evaluation of $P_{N1}(y)$ by this method using a digital computer is however excessively time consuming and the alternative approximate algorithm, which is the subject of this Appendix, has been used for the iterative generation of $P_{N1}(y)$ from $P_1(x)$ and $P_{(N-1)1}(x)$.

It is convenient to descibe this algorithm in relation to the derivation of $P_{N1}(y)$ which is the probability density function of the average of the squares of N samples taken at random from the same pure sine wave. Any particular value of the sum of the squares of N random samples taken from this sine wave will be denoted by $\psi(N)$ where

$$\psi(N) = \sum_{n=1}^{N} \sin^2 \phi_n$$

ϕ_n is taken from ϕ which is an evenly distributed random number in the range $0 \leq \phi_n \leq \pi/2$.

The range of $\psi(N)$ is

$$0 \leq \psi(N) \leq N$$

In order to combine $P_{(N-1)1}(y)$ with $P_{11}(y)$ to produce $P_{N1}(x)$ it is necessary to split the ranges of $\psi(1)$ and $\psi(N-1)$ into NB bands of equal width. The use of 500 such bands gives very good convergence in this case.

$P_{N1}(y)$, which is a continuous function, may thus be represented discretely by NB terms of the form ${}_NP_m, 1 \leq m \leq NB$, where ${}_NP_m$ is defined as the probability that $\psi(N)$ will fall in band number m. The range of values of $\psi(N)$ covered by ${}_NP_m$ is defined by

$$(m-1)Nh \leq \psi(N) \leq mNh \quad (h = 1/NB)$$

and $P_{N1}(y)$ is related to ${}_NP_m$ by the expression

$$ {}_NP_m = P_{N1}((m-\tfrac{1}{2})Nh).Nh $$

To create ${}_NP_r$ from $P_{11}(y)$ and $P_{(N-1)1}(y)$, the following procedure has been adopted.

The range of values of $\psi(N)$ covered by ${}_NP_r$ is known to be

$$ (r-1)Nh \leqslant \psi(N) \leqslant rNh $$

For each n, $1 \leqslant n \leqslant NB$, the range of values of $\psi(N-1)$ covered by ${}_{N-1}P_n$ is known to be

$$ (n-1)(N-1)h \leqslant \psi(N-1) \leqslant n(N-1)h $$

and for each m, $1 \leqslant m \leqslant NB$, the range of values of $\psi(1)$ covered by ${}_1P_m$ is known to be

$$ (m-1)h \leqslant \psi(1) \leqslant mh $$

If the two probabilities ${}_{N-1}P_n$ and ${}_1P_m$ are multiplied together, the range of values of $\psi(N)$ covered by the product is given by

$$ (n-1)(N-1)h + (m-1)h \leqslant \psi(N) \leqslant n(N-1)h + mh $$

If this range overlaps the range of ${}_NP_r$ by an amount X_{mn}, then the contribution to ${}_NP_r$ from the combination of ${}_{N-1}P_n$ and ${}_1P_m$ is defined as

$$ \frac{X_{mn}}{rNh-(r-1)Nh} \cdot {}_{N-1}P_n \cdot {}_1P_m $$

If the value of X_{mn} is negative, that is the two ranges do not overlap, X_{mn} is set to zero.

This process is repeated for all possible values of n, m and r yielding

$$ {}_NP_r = \sum_{n=1}^{NB} \sum_{m=1}^{NB} \frac{X_{nm}}{Nh} \cdot {}_{N-1}P_n \cdot {}_1P_m $$

Successive, iterative application of this algorithm thus enables $P_{N1}(y)$ to be calculated for any value of N using $P_{11}(y)$ as the only input.

A.1 Checks on calculation algorithm accuracy.

In order to establish the validity of the calculation algorithm both theoretical and practical checks have been carried out.

The theoretical check was performed by using the calculation algorithm to generate iteratively the chi-squared distribution for N degress of freedom $1 \leq N \leq 16$, using as the only input, the chi-squared distribution for one degree of freedom in the range $0 \leq \chi^2 \leq 20$. For each value of N, the calculated distribution has been compared with the theoretical chi-squared distribution for N degrees of freedom given by

$$P_N(\chi^2) = \frac{1}{\Gamma(\frac{N}{2})\ 2^{\frac{1}{2}N}} \cdot (\chi^2)^{\frac{1}{2}N-1}\ e^{-\frac{1}{2}\chi^2}$$

Figures A1 and A2 show typical comparisons between theoretical and calculated values for N = 4, 16 respectively. The agreement between the theoretical and calculated data is remarkably good since this check applies stringent conditions in that the range of values for chi-squared is strictly infinite whereas the calculation algorithm can only accept data in a finite range of values.

As a practical check of the calculation algorithm, values of $P_{N1}(x)$ have also been derived by digital simulation. Figures A3 and A4 show typical comparisons between data derived by the two methods for N = 3, 16. The minimal lack of agreement is due to slight uneveness in the random number generator used for the digital simulation.

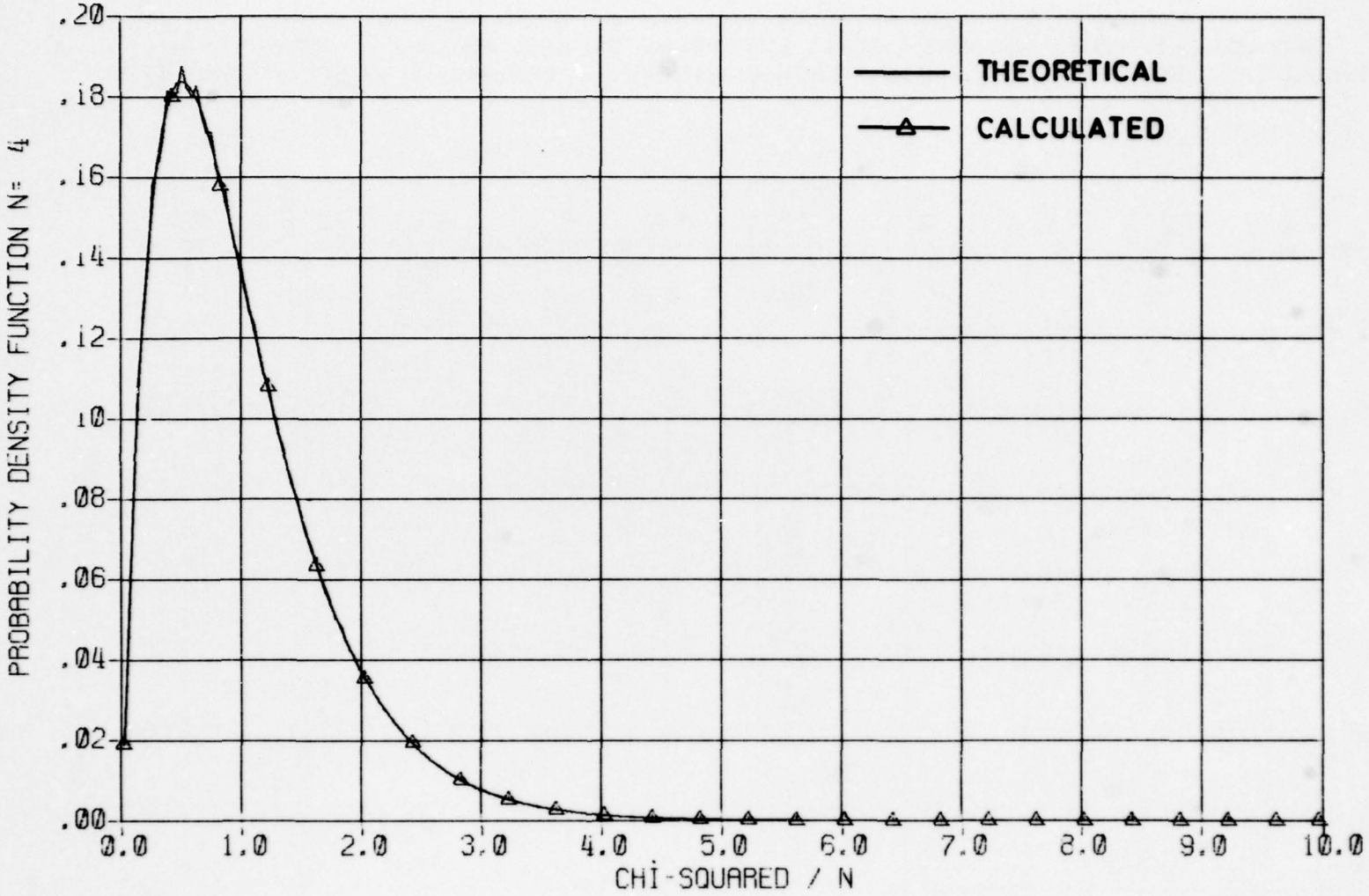

FIG. A1 COMPARISON OF THEORETICAL PROBABILITY DENSITY FUNCTION OF CHI-SQUARED DISTRIBUTION FOR 4 DEGREES OF FREEDOM WITH THE PROBABILITY DENSITY FUNCTION CALCULATED FOR THE SAME DISTRIBUTION USING THE ITERATIVE ALGORITHM DESCRIBED IN APPENDIX

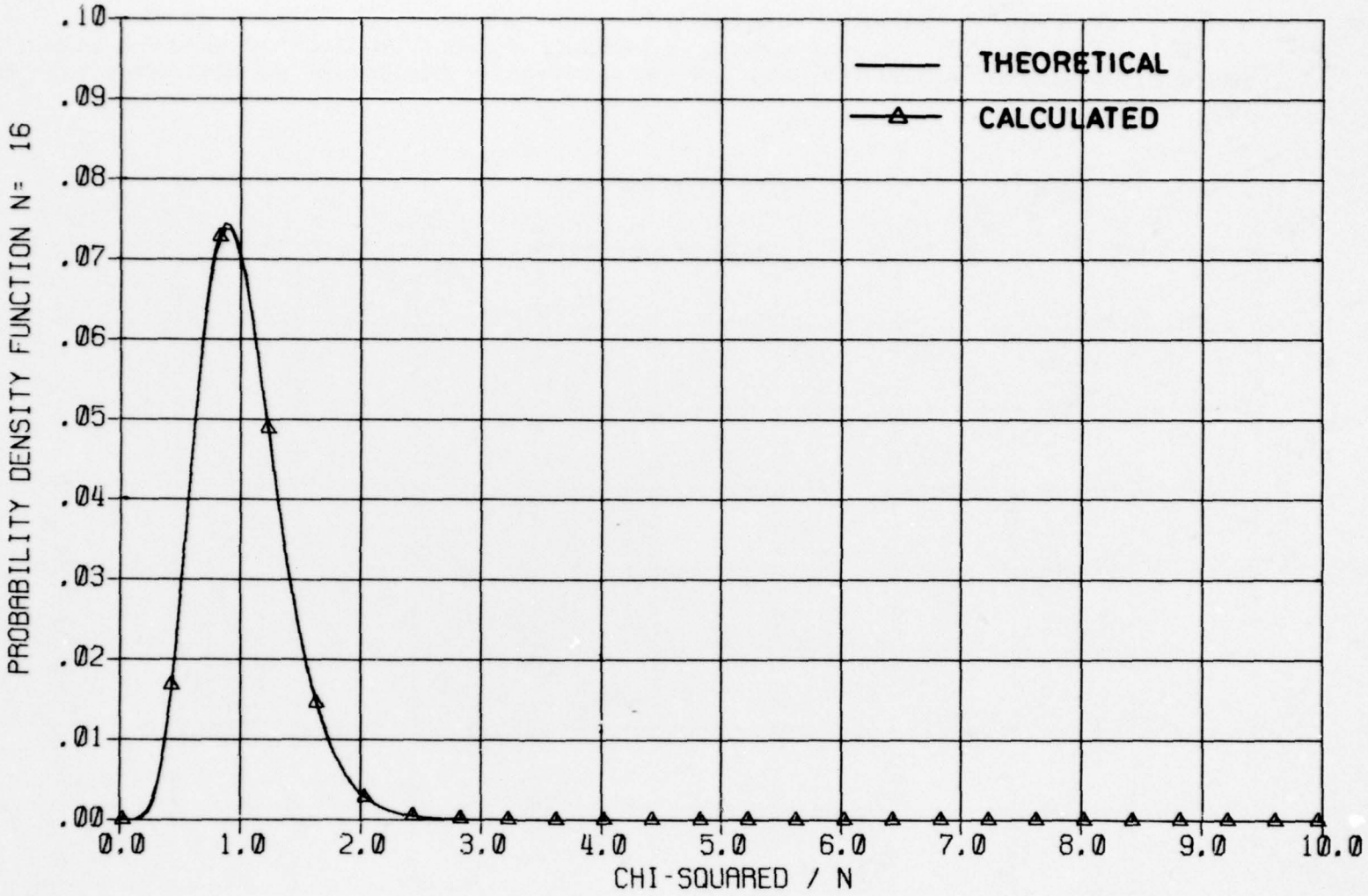

FIG. A2 COMPARISON OF THEORETICAL PROBABILITY DENSITY FUNCTION OF CHI-SQUARED DISTRIBUTION FOR 16 DEGREES OF FREEDOM WITH THE PROBABILITY DENSITY FUNCTION CALCULATED FOR THE SAME DISTRIBUTION USING THE ITERATIVE ALGORITHM DESCRIBED IN APPENDIX

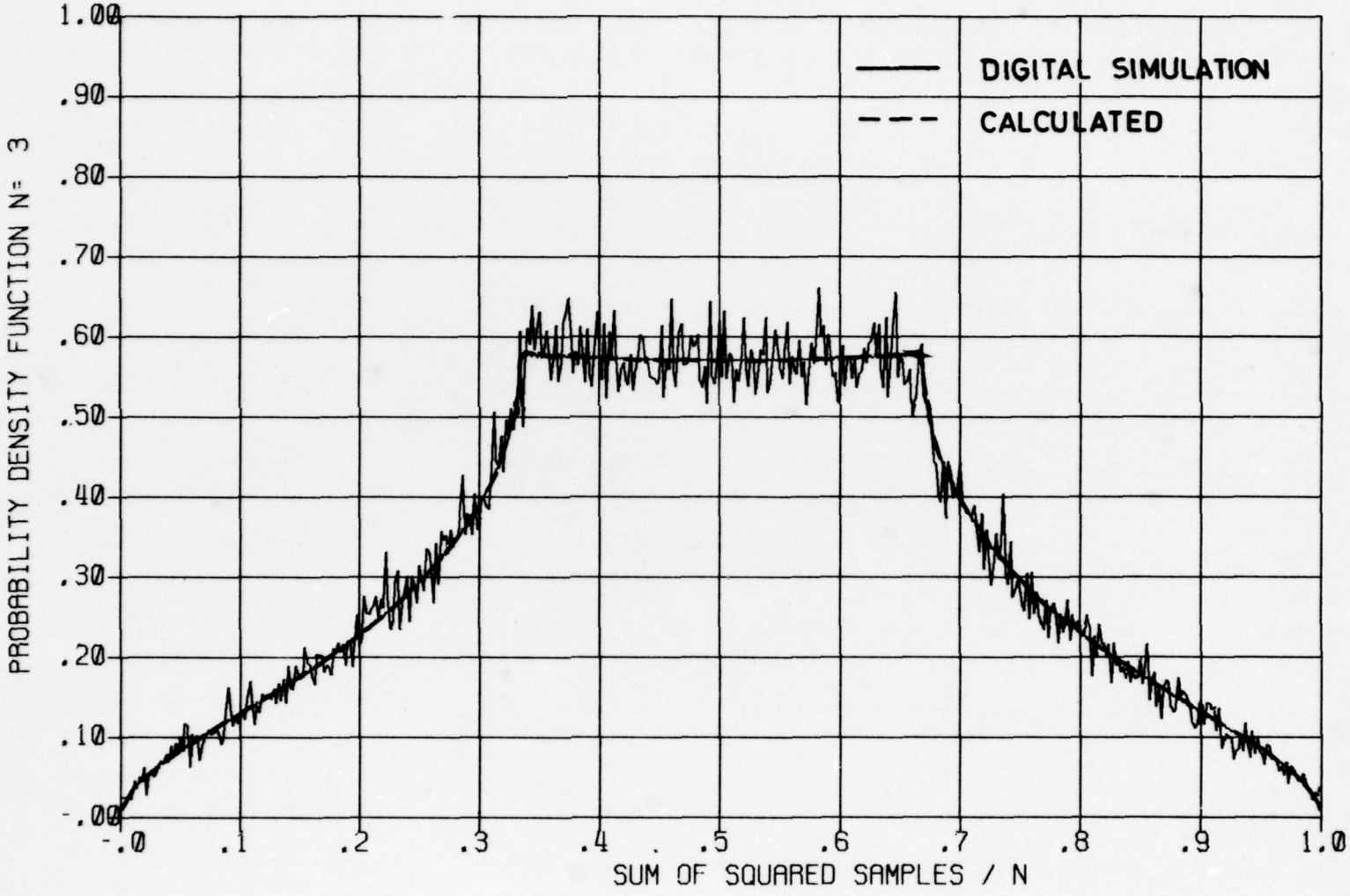

FIG. A3 PROBABILITY DENSITY FUNCTION OF THE AVERAGE OF THE SQUARES OF 3 SAMPLES TAKEN RANDOMLY FROM A SINGLE PURE SINE WAVE. RESULTS OF INDEPENDENT ESTIMATIONS BY DIGITAL SIMULATION AND BY ITERATIVE USE OF THE ALGORITHM DESCRIBED IN APPENDIX

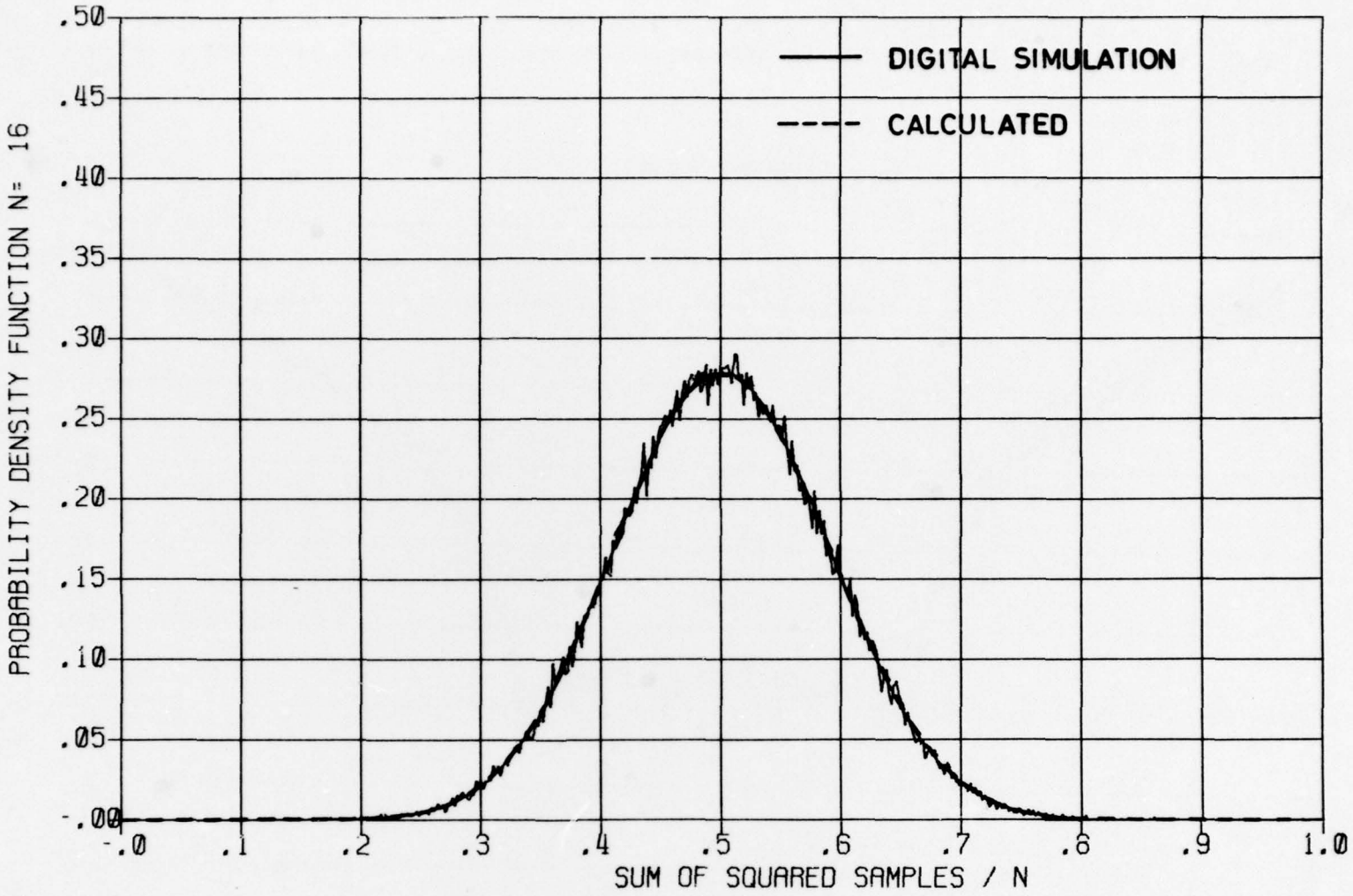

FIG. A4 PROBABILITY DENSITY FUNCTION OF THE AVERAGE OF THE SQUARES OF 16 SAMPLES TAKEN RANDOMLY FROM A SINGLE PURE SINE WAVE. RESULTS OF INDEPENDENT ESTIMATIONS BY DIGITAL SIMULATION AND BY ITERATIVE USE OF ALGORITHM DESCRIBED IN APPENDIX